

Revisiting Q-ball Interactions with Matters

Ayuki Kamada^a, Takumi Kuwahara^b, and Keiichi Watanabe^c

^a *Institute of Theoretical Physics, Faculty of Physics, University of Warsaw, ul. Pasteura 5, PL-02-093 Warsaw, Poland*

^b *Center for High Energy Physics, Peking University, Beijing 100871, China*

^c *Institute for Cosmic Ray Research, The University of Tokyo, Kashiwa, Chiba 277-8582, Japan*

Abstract

Q-ball dark matter is one of candidates for the macroscopic dark matter: Q-ball is a non-topological solitonic configuration, whose stability can be ensured by global charge and energy conservation. One of the crucial factors for discovering signatures from the Q-ball dark matter, is the interactions of the Q-ball dark matter with ordinary matter. In particular, the scattering of ordinary matter off the Q-ball dark matter is important for the direct detection searches, such as paleo-detectors. It was conjectured that quarks incident on the Q-ball were reflected as anti-quarks with a probability of order unity, but it costs the energy of the squark in the Q-ball, which cannot be paid in the scattering of ordinary matter off the Q-ball dark matter. In addition, once a proton is reflected as an anti-proton, the Q-ball obtains the electromagnetic charge. In this study, we revisit the scattering process of quarks with the Q-ball with taking into account the energy cost of the scattering and the electromagnetic charge-up of the Q-ball.

1 Introduction

Much of particle nature of dark matter (DM) still remains unrevealed even though the cosmological observations have established the existence of DM. For several decades, many experiments and observations have focused on the weakly interacting massive particles (WIMP) as one of the plausible candidates of the particle DM. Despite the best efforts of the experiments, no crucial evidence for the WIMP paradigm has been shown up. Macroscopic DM is one of the candidates for DM models beyond WIMP paradigm, and it requires for alternative methods searching for macroscopic DM. Q-ball DM is one of candidates for the macroscopic DM (with a mass of $\mathcal{O}(1)$ g and a radius of $\mathcal{O}(10)$ fm [1]): Q-ball is a non-topological solitonic (spherically symmetric) configuration [2–4], whose stability can be ensured by global charge and energy conservation. Supersymmetric extensions of the standard model (SM) may have stable Q-ball (in particular, with gauge-mediated supersymmetry breaking) [5, 6]. One of scalar counterparts of quarks and leptons (squarks and sleptons) gets a field value along a flat direction of the scalar potential [7, 8].

Interactions of Q-ball DM with matter are crucial keys for discovering signals from the Q-ball at experiments and observations. There are several studies about the Q-ball interaction: decay into ordinary matter [9–12] and absorption of baryons [13]. In particular, scattering with nucleons is important for direct detection searches for Q-ball DM. It was conjectured in Ref. [14] that the Q-ball absorbs nucleons during the scattering. There, a scalar field gets its field value inside the Q-ball, and its value gradually decreases towards the outer of the Q-ball. The scalar field gets a relatively small field value near the boundary of the Q-ball, where the quark mass from the field value can be smaller than the quantum chromodynamics (QCD) dynamical scale and the color symmetry is broken by the field value. Then, the nucleons incident on the Q-ball are dissociated into quarks on the layer, and the energy of nucleons can be released by emitting pions [14, 15]. Through the annihilation process of the incident quark into the scalars inside the Q-ball, nucleons are absorbed on the Q-ball. Meanwhile, the scattering of Q-ball with the ordinary matter has been considered from the quantum-mechanical perspective in Refs. [9, 16, 17]. In Ref. [17], the Q-ball is considered as the static background, and we find that quarks incident on the Q-ball are reflected as anti-quarks with a probability of order unity. It leads to quick energy release through annihilation of the reflected anti-quarks with the surrounded materials. However, after the nucleon (quark)–Q-ball scattering, the squarks should be added in the Q-ball in accordance with the baryon number conservation, and it costs the energy of squarks in the Q-ball, which we refer to as the chemical potential ω . When the scattering process cannot pay the energy cost, the nucleon (quark) cannot be reflected as the anti-nucleon (anti-quark). In addition, once a proton is reflected as an anti-proton, the Q-ball obtains the electromagnetic charge. In the literature, it has not been taken into account to pay the energy cost and to charge up due to scattering with nucleons. In this study, we revisit the scattering process of quarks with the Q-ball with incorporating these effects. We focus on the Q-ball with the udd flat direction, which carries only the baryon number.

Recently, a new avenue has been proposed for direct searches of DM using ancient mineral as target materials, so-called paleo detector [18, 19]. Instead of constructing detectors with a large target mass as conventional direct detection experiments, ancient minerals can record scratches from the DM-nucleon scattering for quite long time scale, about a billion years. For the material of 1 kg recorded for about a billion years, the exposure for this kind of experiments can achieve to the same orders of that for conventional direct detection experiments with the target mass of 10^4 kg achieved in a year. As for the macroscopic DM, it is challenging to explore the recoil signals from the DM-

nucleon scattering in the conventional direct detection experiments since the DM flux coming into a detector in an order of years is limited. Meanwhile, the paleo-detector is a good candidate for the direct detection experiments searching for macroscopic DM since they have recorded the recoil signals for a billion years. In Ref. [19], the case of the electromagnetically-charged Q-ball [20–23] has been discussed: due to the high energy loss of the charged Q-ball in materials, the expected tracks would be longer than the WIMP-induced tracks. Even for the electromagnetically-neutral Q-ball, there exist the constraints on the flux from experiments searching for absorption of nucleon into Q-ball [1, 15, 20, 24]. It is also expected that the Q-ball would leave unique signals in ancient minerals if incident quarks would be reflected as anti-quarks and would lead to energy release through the pair-annihilation as shown in Ref. [17].

This paper is organized as follows: In Section 2, we revisit scattering of Q-ball DM with quarks in the presence of the chemical potential for the cases of scattering on the infinitely large Q-ball wall in Section 2.1, and then we discuss the three-dimensional scattering in Section 2.2. We discuss the implication of the quark scattering to the nucleon scattering in Section 3. Section 4 is devoted to concluding our study.

2 Scattering of Quarks

In this section, we revisit quark scattering under a Q-ball background oscillating in time (in contrast to that under the static Q-ball background in Ref. [17]). We first review the basics of Q-ball scattering and summarize our notation: we consider a toy model that describes scattering of quark without the color degrees of freedom with Q-ball. Then, we discuss the scattering of quark with infinitely large Q-ball wall and the three-dimensional scattering with finite-size Q-ball.

Let us consider a toy model in which we disregard the color degrees of freedom and that captures the key features of fermion scattering under a Q-ball background. In the next section, we discuss the implication of analysis in this section to a realistic setup. Although we do not take into account the color degrees of freedom, we utilize the same names for the fields as in the supersymmetric models. The squarks φ that have a flat direction couples to the quark ψ and the gluino λ . We here use two-component notation for fermions. The relevant parts of the Lagrangian are

$$\mathcal{L} = -\sqrt{2}g_s(\lambda\psi_i\varphi_i^*) + \text{h.c.}, \quad (2.1)$$

where g_s denotes a gauge coupling constant and $i = 1, 2$ represents flavor indices. λ denotes gluino that does not have its own charge, and ψ_1 and ψ_2 have the opposite charges. The Majorana mass term for gluino is

$$\mathcal{L}_M = M_\lambda\lambda\lambda. \quad (2.2)$$

Here, the Majorana mass is assumed to be real-valued.

The squarks obtain a non-zero field value $\langle\varphi_i\rangle = \varphi_{i,0} \neq 0$ in the Q-ball background, then the quark gets a mass mixing with gluino. The mass matrix for fermions in the Q-ball background is parametrized as

$$M_\psi = \begin{pmatrix} 0 & 0 & M_1 \\ 0 & 0 & M_2 \\ M_1 & M_2 & M_\lambda \end{pmatrix}. \quad (2.3)$$

Here, $M_{1(2)}$ denotes the mass mixing between quark ψ_1 (ψ_2) and gluino. We assume that the Dirac mass of quarks is negligible compared to the other mass parameters, the gluino mass and the field values of the squark fields. We introduce the mixing angles α, β and the dimensionful parameter M , and the mass parameters are written as

$$\begin{aligned} M_1 &= \overline{M} \cos \alpha, & M_2 &= \overline{M} \sin \alpha, \\ \overline{M} &= M \sin 2\beta, & M_\lambda &= 2M \cos 2\beta. \end{aligned} \quad (2.4)$$

Here, α denotes the ratio of the field values of the squark fields: $\tan \alpha = \varphi_{1,0}/\varphi_{2,0}$. The field rotation by α makes only a linear combination of the fermions, which is denoted by ψ , to couple to the gluino.

$$\begin{pmatrix} \psi_1 \\ \psi_2 \end{pmatrix} = \begin{pmatrix} \sin \alpha & \cos \alpha \\ -\cos \alpha & \sin \alpha \end{pmatrix} \begin{pmatrix} \chi_0 \\ \psi \end{pmatrix}. \quad (2.5)$$

Here, χ_0 denotes another linear combination, which does not have a mass mixing with the gluino. The gluino and the massive combination of quarks mix with each other with the mixing angle β . Then, the mass eigenstates of fermions are given by the rotation from the basis (ψ, λ) as follows.

$$\begin{pmatrix} \psi \\ \lambda \end{pmatrix} = \begin{pmatrix} \cos \beta & \sin \beta \\ -\sin \beta & \cos \beta \end{pmatrix} \begin{pmatrix} \chi_1 \\ \chi_2 \end{pmatrix}. \quad (2.6)$$

Here, χ_1 and χ_2 denote the mass eigenstates with the Majorana masses $-M_- = -2M \sin^2 \beta$ and $M_+ = 2M \cos^2 \beta$, respectively.

Now, we consider wave functions for fermions inside and outside the Q-ball. As far as the Dirac mass terms for quarks are negligible, quark ψ and gluino λ outside the Q-ball obey the following equations.

$$\begin{cases} i\bar{\sigma} \cdot \partial \psi = 0, \\ i\bar{\sigma} \cdot \partial \lambda - M\lambda^\dagger = 0, \end{cases} \quad (2.7)$$

where $\lambda^\dagger = i\sigma^2 \cdot \lambda^*$. M denotes the Majorana mass for gluinos. Meanwhile, quark and gluino have the mass term proportional to the field value of the squark field φ inside Q-ball. Thus, wave functions for quark and gluino inside Q-ball obey the following equations.

$$\begin{cases} i\bar{\sigma}^\mu \partial_\mu \psi - \varphi \lambda^\dagger = 0, \\ i\bar{\sigma}^\mu \partial_\mu \lambda - M\lambda^\dagger - \varphi \psi^\dagger = 0. \end{cases} \quad (2.8)$$

Let us consider the squark field oscillating in time, $\varphi = \varphi_0 e^{-i\omega t}$. A time-dependent phase factor appears in the mass term, but the phase factor will be removed by the field redefinition $\psi = e^{-i\omega t} \psi_0$. The equations will be reduced as follows.

$$\begin{cases} i\bar{\sigma}^\mu \partial_\mu \psi_0 + \omega \bar{\sigma}^0 \psi_0 - \varphi_0 \lambda^\dagger = 0, \\ i\bar{\sigma}^\mu \partial_\mu \lambda - M\lambda^\dagger - \varphi_0 \psi_0^\dagger = 0. \end{cases} \quad (2.9)$$

There is an extra term proportional to ω in the equation for ψ_0 . The chemical potential ω is typically much smaller than the field value φ and the gluino mass M . In the following, we obtain the wave

functions by solving the equation with ignoring the ω term, and the oscillating phase factor appears only in the matching conditions for the wave function of the matter fermions.

Finally, we comment on the four-component notations for fermions in the Weyl representation. The four-component Majorana fermions for quark are written as

$$\Psi_W^{\text{in}} = \begin{pmatrix} e^{-i\omega t}\psi_0 \\ e^{i\omega t}\psi_0^\dagger \end{pmatrix}, \quad \Psi_W^{\text{out}} = \begin{pmatrix} \psi \\ \psi^\dagger \end{pmatrix}, \quad (2.10)$$

where the superscripts, “in” and “out”, indicate the quarks inside and outside the Q-ball, respectively. We note that the phase factor appears only for the quarks inside the Q-ball. The four-component fermions for gluinos are defined in a similar way to Ψ_W^{out} , namely the four-component fermion without the time-dependent phase factor, for both inside and outside the Q-ball.

2.1 Scattering on the infinitely large Q-ball wall

We begin to discuss the (colorless) quark wave functions and their matching conditions for the scattering on the infinitely large Q-ball wall. We assume that Q-ball boundaries are located at $z = \pm R$ and are infinitely extended in other directions as shown in Fig. 1. The fermions get massive in $|z| < R$ through the field value of squarks. A Majorana fermion ψ , collectively denoting quarks and gluinos outside Q-ball and massive fermions inside Q-ball, obeys the following equation:

$$i\vec{\sigma} \cdot \partial \psi - iM\sigma^2\psi^* = 0, \quad (2.11)$$

where M is the Majorana mass. A solution for the equation is given by

$$\begin{cases} \psi = \sqrt{p \cdot \sigma} (Ae^{-ip \cdot x} - i\sigma^2 A^* e^{ip \cdot x}), & M > 0, \\ \psi = \sqrt{p \cdot \sigma} (Ae^{-ip \cdot x} + i\sigma^2 A^* e^{ip \cdot x}), & M < 0, \end{cases} \quad (2.12)$$

Here, A denotes an arbitrary two-component spinor, and $p = (E, \vec{p})$ with $\vec{p}^2 = E^2 - M^2$. As for the Majorana fermions inside the Q-ball, the injected energy E is less than masses of Majorana fermions, namely $E < M$. For such a case, we consider the wave functions with an analytic-continued momentum p . We use the wave function with the analytic-continued momentum given by

$$\begin{cases} \psi = \sqrt{p \cdot \sigma} A e^{-ip \cdot x} + \sqrt{p^* \cdot \sigma} (-i\sigma^2) A^* e^{ip^* \cdot x}, & M > 0, \\ \psi = \sqrt{p \cdot \sigma} A e^{-ip \cdot x} - \sqrt{p^* \cdot \sigma} (-i\sigma^2) A^* e^{ip^* \cdot x}, & M < 0. \end{cases} \quad (2.13)$$

We summarize several formulae regarding the analytic-continued wave functions in Appendix A.

There are five kinds of fermions in the matching conditions for the fermions at the Q-ball boundaries. The incoming quark (whose wave function is denoted by ψ_A) enters the Q-ball from $z < -R$, and there are the reflected quark (ψ_B) in $z < -R$ and the transmitted quark (ψ_C) in $z > R$. When the energy of the incoming quark is large enough, there are the reflected gluino (λ_B) and the transmitted gluino (λ_C). The matching conditions of wave functions at the Q-ball boundary $z = -R$ are

$$\psi_A + \psi_B = \sum_{\pm} (\sin \beta \chi_D^{\pm} + \cos \beta \chi_F^{\pm}), \quad \lambda_B = \sum_{\pm} (\cos \beta \chi_D^{\pm} - \sin \beta \chi_F^{\pm}). \quad (2.14)$$

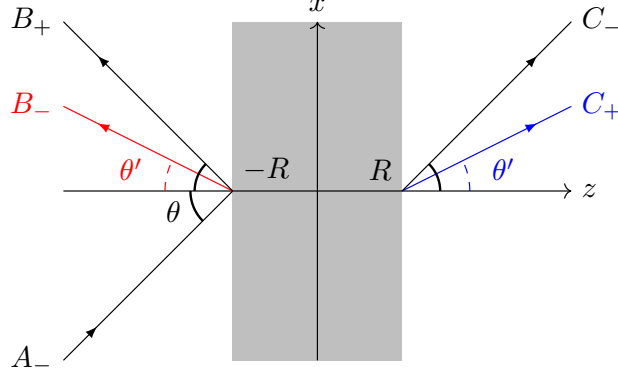


Figure 1: Scattering on the infinitely large Q-ball wall with the left-handed quark coming in: the shaded area corresponds to the Q-ball. The black solid lines depict the incoming, reflected, and transmitted quarks with the energy of E , while the colored lines depict the reflected and transmitted quarks with the energy of $E - 2\omega$. Since the energy E is much less than the masses of the fermions inside the Q-ball, the massive fermions are assumed to run on the z -axis and the transmitted fermions are emitted from the z -axis.

Here, $\chi_{D,F}^{\pm}$ denote the wave functions for the Majorana fermions inside the Q-ball: χ_D^{\pm} denotes the fermion with the mass of M_+ , while χ_F^{\pm} denotes the fermion with the mass of M_- . The superscript of $\chi_{D,F}^{+(-)}$ indicates the growing (decaying) mode. The matching conditions at another Q-ball boundary $z = R$ are:

$$\psi_C = \sum_{\pm} (\sin \beta \chi_D^{\pm} + \cos \beta \chi_F^{\pm}), \quad \lambda_C = \sum_{\pm} (\cos \beta \chi_D^{\pm} - \sin \beta \chi_F^{\pm}). \quad (2.15)$$

Now, we obtain the spinor relations among the fermions for given spinor of the incoming fermion, A . We focus only on positive and negative helicities for A and find the relations for each helicity, but we obtain the generic relations by combining the relations for each helicity.

In this subsection, we consider the case that the incoming quark comes into the Q-ball wall with an oblique angle θ : θ denotes the angle between the z axis and the momentum of the incoming quark. We assume that the momenta lie in the x - z plane as illustrated in Fig. 1. Assuming the helicity of the incoming quark, we construct the other spinors by solving the matching conditions. We decompose the spinors for the massless quarks and assign the momenta for all fermions, again. First, we consider the case that the left-handed quark comes in. The four-momenta for massless quarks are assigned as follows:

$$\begin{aligned} p &= (E, E \sin \theta, 0, E \cos \theta), \\ p_{B+} &= (E, E \sin \theta, 0, -E \cos \theta), \quad p_{B-} = (E - 2\omega, (E - 2\omega) \sin \theta', 0, -(E - 2\omega) \cos \theta'), \\ p_{C+} &= (E - 2\omega, (E - 2\omega) \sin \theta', 0, (E - 2\omega) \cos \theta'), \quad p_{C-} = (E, E \sin \theta, 0, E \cos \theta). \end{aligned} \quad (2.16)$$

Here, we decompose the massless fermions into components with definite spin directions (denoted by the label \pm), so that their spinors projected onto the z -axis satisfy the proper projection operation, discussed later. We assume the energy to be E for the left-handed quarks, B_+ and C_- , while the energy to be $E - 2\omega$ for the right-handed anti-quarks, B_- and C_+ due to the energy cost for adding the left-handed squarks in the Q-ball. Meanwhile, we do not decompose the massive fermions into

each spinor part since both spinors with different spins are assumed to have the same energy for them.

$$\begin{aligned}\kappa_B &= (E - \omega, E \sin \theta, 0, -iM), & \kappa_C &= (E - \omega, E \sin \theta, 0, iM), \\ \kappa_D^\pm &= (E - \omega, E \sin \theta, 0, \mp iM_\pm), & \kappa_F^\pm &= (E - \omega, E \sin \theta, 0, \mp iM_-).\end{aligned}\quad (2.17)$$

Here, we take the limit that the mass parameters M and M_\pm are much larger than the injected energy E and the chemical potential ω .

The massless fermions with the different energy can be transmitted and reflected with a different angle, denoted by θ' . The momentum conservation in the x -direction gives the following relation between the angles:

$$\frac{\sin \theta'}{\sin \theta} = \frac{E}{E - 2\omega}. \quad (2.18)$$

We note that the scattering is available even when $E \sin \theta > E - 2\omega$ (namely, $\sin \theta' > 1$) once we consider the analytic continuation of θ' as we will see later. The massive fermions also have a momentum in the x direction due to the momentum conservation, but we ignore the momentum unless it is leading order since it is much smaller than the gluino mass and the masses of Majorana fermions inside the Q-ball (see Appendix B for detail). Since the spins of massless quarks are assumed to be aligned into the momentum direction, we impose the projection operation on the spinors projected onto the z -axis as follows.

$$\begin{aligned}\frac{1}{2}(\mathbb{1} + \sigma^3)e^{i\theta\frac{\sigma^2}{2}}A_- &= 0, \\ \frac{1}{2}(\mathbb{1} + \sigma^3)e^{-i\theta'\frac{\sigma^2}{2}}B_- &= 0, & \frac{1}{2}(\mathbb{1} - \sigma^3)e^{-i\theta\frac{\sigma^2}{2}}B_+ &= 0, \\ \frac{1}{2}(\mathbb{1} + \sigma^3)e^{i\theta\frac{\sigma^2}{2}}C_- &= 0, & \frac{1}{2}(\mathbb{1} - \sigma^3)e^{i\theta'\frac{\sigma^2}{2}}C_+ &= 0.\end{aligned}\quad (2.19)$$

Here, we note that the rotation angle of B_- and C_+ is different from others due to the different energy of B_- and C_+ . The matching conditions for the wave functions give the constant spinors in terms of the spinor of the incoming quark A_- . The detail of the calculation is given in Appendix B. In the limit of large $M_{(\pm)}R$, we find the constant spinors for the reflected quark and the transmitted quark as follows.

$$\sqrt{E}e^{-i\theta\frac{\sigma^2}{2}}B_+e^{iER\cos\theta} = \frac{\sin\left(\frac{\theta-\theta'}{2}\right)}{\cos\left(\frac{\theta+\theta'}{2}\right)}(i\sigma^2)\sqrt{E}e^{i\theta\frac{\sigma^2}{2}}A_-e^{-iER\cos\theta}, \quad (2.20)$$

$$\sqrt{E-2\omega}e^{-i\theta'\frac{\sigma^2}{2}}B_-e^{i(E-2\omega)R\cos\theta'} = i\frac{\cos\theta}{\cos\left(\frac{\theta+\theta'}{2}\right)}\sqrt{E}e^{i\theta\frac{\sigma^2}{2}}A_-e^{-iER\cos\theta}, \quad (2.21)$$

$$\sqrt{E-2\omega}e^{i\theta'\frac{\sigma^2}{2}}C_+e^{i(E-2\omega)R\cos\theta} = 2e^{-M_-R}(1+\tan^2\beta)\frac{\cos\theta\sin\left(\frac{\theta-\theta'}{2}\right)}{\cos^2\left(\frac{\theta+\theta'}{2}\right)}\sigma^2\sqrt{E}e^{i\theta\frac{\sigma^2}{2}}A_-e^{-iER\cos\theta}, \quad (2.22)$$

$$\sqrt{E}e^{i\theta\frac{\sigma^2}{2}}C_-e^{iER\cos\theta} = 2e^{-M_-R}(1+\tan^2\beta)\frac{\cos\theta\cos\theta'}{\cos^2\left(\frac{\theta+\theta'}{2}\right)}\sqrt{E}e^{i\theta\frac{\sigma^2}{2}}A_-e^{-iER\cos\theta}. \quad (2.23)$$

We comment on the case with $E \sin \theta > E - 2\omega$, where the quark injects into the Q-ball relatively parallel to the Q-ball surface. Since the incoming quark is just passing through on the Q-ball surface when $\theta = \pi/2$, we naively expect that the incoming quark is elastically reflected in this case. When $E \sin \theta > E - 2\omega$, we can analytically continue the sine function such that $\sin \theta' > 1$, and the analytic-continued cosine function is the pure imaginary. We can easily realize this analytic continuation by choosing $\theta' = \pi/2 - i\eta$ with a positive-real parameter η (namely, $\sin \theta' = \cosh \eta$ and $\cos \theta' = i \sinh \eta$). The prefactor of B_+ is computed as follows.

$$\frac{\sin^2 \left(\frac{\theta - \theta'}{2} \right)}{\cos^2 \left(\frac{\theta + \theta'}{2} \right)} = \frac{1 - \sin \theta \cosh \eta + i \cos \theta \sinh \eta}{1 - \sin \theta \cosh \eta - i \cos \theta \sinh \eta}. \quad (2.24)$$

Hence, the absolute value of the prefactor of B_+ is unity, while the absolute value of the prefactor of B_- is $e^{-i(E-2\omega)R \cos \theta'} = e^{(E-2\omega)R \sinh \eta}$ at the Q-ball boundary. The analytically-continued momentum for B_- is given by

$$p_{B_-} = (E - 2\omega, (E - 2\omega) \cosh \eta, 0, -i(E - 2\omega) \sinh \eta), \quad (2.25)$$

and hence, the right-handed anti-quark B_- is no longer the propagating wave.

The probability flux is defined in terms of the direction normal to the Q-ball surface. In contrast to the previous case, there are two non-zero constant spinors for the reflected quarks, B_{\pm} , while the constant spinors for the transmitted quarks are quite suppressed in the large $M_{(\pm)}R$ limit and we ignore them. Therefore, the probability flux after the scattering consists only of the reflected quarks in this limit, and we find

$$(E - 2\omega) \cos \theta' B_-^\dagger B_- + E \cos \theta B_+^\dagger B_+ = E \cos \theta A_-^\dagger A_- . \quad (2.26)$$

Once we choose the oblique angle to be $\theta = \theta' = 0$, it corresponds to the scattering with normal incident. In the limit of large Q-ball radius R , we find $B_+ = C_+ = 0$ and

$$\sqrt{E - 2\omega} B_- e^{i(E-2\omega)R} = i\sqrt{E} A_- e^{-iER}, \quad (2.27)$$

$$\sqrt{E} C_- e^{iER} = 2(1 + \tan^2 \beta) e^{-2M-R} \sqrt{E} A_- e^{-iER}. \quad (2.28)$$

The spin directions of both the transmitted and reflected quarks are the same as that of the incoming quarks. The momentum of the reflected quark is reversed compared to that of the incoming quark. This implies that the left-handed quark is completely reflected as the right-handed anti-quark as far as $E > 2\omega$. This implies that the left-handed quark is reflected as the right-handed anti-quark as far as $E > 2\omega$. The spinor C_- is suppressed by e^{-2M-R} , and hence the transmission rate is also suppressed in the large R limit. Our results are consistent with Ref. [17] where the authors have treated the Q-ball as the semi-infinite large wall located at $z \geq 0$. Our result implies that baryons coming to the Q-ball at normal incident are reflected as its anti-baryons with the probability of order unity.¹ The Q-ball does not get the angular momentum as far as we treat the Q-ball as a background and impose the spin conservation in the matter side. One may consider the slowly rotating Q-ball [25]

¹In Appendix D, we discuss the non-relativistic scattering of nucleon-anti-nucleon system under the Q-ball background.

as the excited state, and then we may be able to incorporate the spin flip of the incoming quark.²

We can consider the opposite helicity for the incoming quark, namely its spinor satisfying $(\mathbb{1} - \sigma^3)e^{i\theta\frac{\sigma^2}{2}}A_+ = 0$. We obtain the similar result even for this case: the right-handed quark is completely reflected as the left-handed anti-quark when the incoming quark enters the Q-ball at normal incidence. We discuss this case in detail in Appendix B.

We may consider the case where the left-handed incoming quark with the energy of $E - 2\omega < 0$. Since the energy of the reflected quark and the transmitted quark should be positive, the momentum assignment for the quarks, Eq. (2.16), for the case of normal incident ($\theta = \theta' = 0$) should be changed as follows.

$$p_{B-} = (-E + 2\omega, 0, 0, E - 2\omega), \quad p_{C+} = (-E + 2\omega, 0, 0, -E + 2\omega), \quad (2.29)$$

and same as Eq. (2.16) with $\theta = \theta' = 0$ for other quarks. In this case, the positive-frequency solution for B_- matches to the negative-frequency solution of the incoming quark A_- to satisfy the matching conditions at x for any time. We get the constant spinor B_- in the large R limit as follows.

$$\sqrt{2\omega - E}B_-e^{i(2\omega - E)R} = i\sqrt{E}(-i\sigma^2)A_-^*e^{-iER}. \quad (2.30)$$

However, this relation cannot be interpreted as the quantum mechanical scattering process. The unitary evolution of the state does not give this relation. We cannot deal with this process within the scattering problem in the relativistic quantum mechanics and must go beyond to deal with it.

We have considered the scattering of quarks on the Q-ball in the mass basis so far: for the scattering with $\omega = 0$ and normal incident ($\theta = 0$), the quark corresponding to the massive Majorana fermion inside the Q-ball is reflected as the anti-quark, while the quark corresponding to the massless fermion inside the Q-ball just passes through the Q-ball. The S -matrix for the scattering is block-diagonalized with respect to the mass eigenstates:

$$S' = \begin{pmatrix} \mathbf{1}_4 & 0 \\ 0 & S_4 \end{pmatrix}, \quad S_4 = i \begin{pmatrix} 0 & 1 & 0 & 0 \\ 1 & 0 & 0 & 0 \\ 0 & 0 & 0 & 1 \\ 0 & 0 & 1 & 0 \end{pmatrix}. \quad (2.31)$$

Here, the in-state for each block is labelled by the helicity and the moving direction, so there is 4×4 sub-matrix for each block. The upper-left block corresponds to the massless fermion χ_0 inside the Q-ball, while the lower-right block corresponds to the massive Majorana fermion ψ . The detail of the non-trivial matrix S_4 is given in Appendix C. We obtain the S -matrix element in terms of the quarks in the original (interaction) basis by the field rotation.

$$S = \begin{pmatrix} \sin^2 \alpha \mathbf{1}_4 + \cos^2 \alpha S_4 & \cos \alpha \sin \alpha (\mathbf{1}_4 - S_4) \\ \cos \alpha \sin \alpha (\mathbf{1}_4 - S_4) & \cos^2 \alpha \mathbf{1}_4 + \sin^2 \alpha S_4 \end{pmatrix}. \quad (2.32)$$

²We cannot deal with such excitation of Q-ball in quantum-mechanical scattering, and thus approaches beyond ours are required. We can, however, find that the event rate for the process not changing helicity is suppressed in a naive Feynman-diagrammatic estimate of the processes. An incoming quark is reflected as a quark when one squark excitation (the squark field is expanded as its field value and excitation inside the Q-ball as $\varphi = \varphi_0 e^{-i\omega t} + \delta\varphi$) is absorbed and one squark excitation with the angular momentum of $\ell = 1$ is emitted. Therefore, the amplitude for the process is proportional to the energy of incoming quark, which arise from the quark propagator (dressed by the field value φ_0). On the other hand, an incoming quark is reflected as an anti-quark when two squark excitations are emitted with the insertion of Majorana mass of gluino due to the chirality flip.

This indicates that the quark ψ_1 (ψ_2) in the interaction basis can be reflected as not only its anti-quark $\bar{\psi}_1$ ($\bar{\psi}_2$) with the probability of $\cos^2 \alpha$ ($\sin^2 \alpha$) but also the anti-quark of the different species $\bar{\psi}_2$ ($\bar{\psi}_1$) with the probability of $\cos \alpha \sin \alpha$.

2.2 Scattering in Spherical Wave

Finally, we generalize the previous discussion to the three-dimensional scattering of quarks with the finite-size Q-ball. The Q-ball is assumed to be spherically symmetric, and hence we can use the spherical wave states, which are eigenstates of energy and total angular momentum. For spin-zero states, we expand the wave function in terms of the spherical harmonics $Y_{\ell,m}(\theta, \phi)$ with angular coordinates (θ, ϕ) and the eigenvalues of the orbital angular momentum operators L^2 and L_z (denoted by ℓ and m). We use the spin-1/2 analog of the spherical harmonics called the spinor spherical harmonics in this study. We discuss the spinor spherical harmonics in Appendix A.2 in detail. The spinor spherical harmonics is a simultaneous eigenfunction of the total angular momentum J^2 and J_z , the orbital angular momentum L^2 , and the spin S^2 . The spinor spherical harmonics is given in a two-component spinor form by

$$\Omega_{\ell \pm \frac{1}{2}, \ell, m}(\theta, \phi) = \frac{1}{\sqrt{2\ell+1}} \begin{pmatrix} \pm \sqrt{\ell \pm m + 1/2} Y_{\ell, m - \frac{1}{2}}(\theta, \phi) \\ \sqrt{\ell \mp m + 1/2} Y_{\ell, m + \frac{1}{2}}(\theta, \phi) \end{pmatrix}. \quad (2.33)$$

Here, the first subscript corresponds to the quantum number of J^2 , $j = \ell \pm 1/2$. ℓ denotes the quantum number of L^2 , while m denote the quantum number of J_z . The spinor for given quantum numbers j and m is decomposed into the radial part and the angular part.

$$\psi_{j,m}(\mathbf{r}) = \frac{1}{r} \begin{pmatrix} iP_\kappa(r) \Omega_{j,j \pm 1/2, m}(\theta, \phi) \\ Q_\kappa(r) \Omega_{j,j \mp 1/2, m}(\theta, \phi) \end{pmatrix} \equiv \frac{1}{r} \begin{pmatrix} ip_{\kappa,m}(\mathbf{r}) \\ q_{\kappa,m}(\mathbf{r}) \end{pmatrix}. \quad (2.34)$$

Here, we introduce a label $\kappa = \mp(j + 1/2)$ (for $j = \ell \pm 1/2$) for the eigenvalues of an operator $K = -1 - 2\mathbf{L} \cdot \mathbf{S}$ associated with the spin-orbit coupling. For a free Dirac fermion, the radial functions $P_\kappa(r)$ and $Q_\kappa(r)$ satisfy the coupled differential equations:

$$\begin{aligned} MP_\kappa + \left(\frac{d}{dr} - \frac{\kappa}{r} \right) Q_\kappa &= EP_\kappa, \\ - \left(\frac{d}{dr} + \frac{\kappa}{r} \right) P_\kappa - MQ_\kappa &= EQ_\kappa. \end{aligned} \quad (2.35)$$

Here, E is the energy of the Dirac fermion, and M denotes the mass of the Dirac fermion. When the scalar background is oscillating, $\varphi = \varphi_0 e^{-i\omega t}$, the wave function inside the Q-ball absorbs the phase factor by the field redefinition. The time-dependent wave function for the four-component Majorana fermions in the Dirac representation (with energy E) are written as follows.

$$\Psi_{j,m}^{\text{in}}(\mathbf{r}, t) = \frac{e^{-iEt}}{r} e^{i\omega t \gamma_5} \begin{pmatrix} ip_{\kappa,m}(\mathbf{r}) \\ q_{\kappa,m}(\mathbf{r}) \end{pmatrix}, \quad \Psi_{j,m}^{\text{out}}(\mathbf{r}, t) = \frac{e^{-iEt}}{r} \begin{pmatrix} ip_{\kappa,m}(\mathbf{r}) \\ q_{\kappa,m}(\mathbf{r}) \end{pmatrix}. \quad (2.36)$$

We also have the charge-conjugated part inside and outside Q-ball. Once we obtain the solution for the matching conditions among $\Psi_{j,m}^{\text{in,out}}$, it is trivial that the charge-conjugated part satisfy the

matching condition. Hence, we consider the matching conditions for the Dirac spinors $\Psi_{j,m}^{\text{in,out}}$ in the following.

We assign different momenta for different massless quarks with the different helicity similar to the previous two sections. Summing a specific linear combination over κ gives a definite chirality of the plane-wave solution for a massless fermion (shown in Appendix A.2). We define the wave functions leading to definite chirality after the summation as follows.

$$\Psi_{+,j,m} = \frac{e^{-iEt}}{r} \begin{pmatrix} ip_{\varkappa,m}(\mathbf{r}) + ip_{-\varkappa,m}(\mathbf{r}) \\ q_{\varkappa,m}(\mathbf{r}) + q_{-\varkappa,m}(\mathbf{r}) \end{pmatrix}, \quad \Psi_{-,j,m} = \frac{e^{-iEt}}{r} \begin{pmatrix} -ip_{\varkappa,m}(\mathbf{r}) + ip_{-\varkappa,m}(\mathbf{r}) \\ -q_{\varkappa,m}(\mathbf{r}) + q_{-\varkappa,m}(\mathbf{r}) \end{pmatrix}, \quad (2.37)$$

Here, \varkappa is positive integer, and \pm indicates the chirality.

The incoming quark is assumed to have a definite chirality as before, and we construct other fermions by solving the matching conditions for the wave functions at the Q-ball boundary ($r = R$). The wave functions inside Q-ball should be regulated at the origin, while the wave functions outside Q-ball should be regulated at large r . In contrast to the previous subsections, we have only to take into account the one wave function inside Q-ball for each massive fermion with a specific chirality and m . Thus, the matching conditions for the wave functions at $r = R$ are

$$\Psi_A + \sum_{m,\pm} \Psi_{B_{\pm,m}} = \sum_{m,\pm} (\sin \beta X_{D_{\pm,m}} + \cos \beta X_{F_{\pm,m}}), \quad (2.38)$$

$$\sum_{m,\pm} \Lambda_{C_{\pm,m}} = \sum_{m,\pm} (\cos \beta X_{D_{\pm,m}} - \sin \beta X_{F_{\pm,m}}). \quad (2.39)$$

Here, the index for j is implicit. Ψ_A denotes the wave function for the incoming quark with a definite chirality and the quantum number m . $\Psi_{B_{\pm,m}}$ and $\Lambda_{C_{\pm,m}}$ are the wave functions for the reflected quark and gluino, respectively. $X_{D,F_{\pm,m}}$ denotes the wave functions for the massive fermions inside Q-ball.

Now, we consider a left-handed chirality for the incoming quark (with $m = -1/2$). We assume the four-momentum of each fermions as follows.

$$\begin{aligned} p &= (E, -E\hat{\mathbf{r}}), & p_{B_{+,m}} &= (E - 2\omega, (E - 2\omega)\hat{\mathbf{r}}), & p_{B_{-,m}} &= (E, E\hat{\mathbf{r}}), \\ \kappa_{C_{\pm,m}} &= (E - \omega, iM\hat{\mathbf{r}}), & \kappa_{D_{\pm,m}} &= (E - \omega, iM_{\pm}\hat{\mathbf{r}}), & \kappa_{F_{\pm,m}} &= (E - \omega, iM_{\pm}\hat{\mathbf{r}}). \end{aligned} \quad (2.40)$$

The outgoing and incoming Dirac fermions are described by the spherical Hankel functions $h_{\kappa}^{(1)}(x)$ and $h_{\kappa}^{(2)}(x)$, which behave as e^{ix}/x and e^{-ix}/x at large x , respectively. We choose the overall coefficients of P_{κ} and Q_{κ} to be convenient for constructing the plain-wave solution in terms of the spinor spherical harmonics. Therefore, the radial functions for the massless quarks for $\varkappa > 0$ ($j = \ell + 1$) are

$$iP_{\varkappa}^{A-} = -i\sqrt{E}rh_{\varkappa}^{(2)}(Er)A_{-}, \quad Q_{\varkappa}^{A-} = \sqrt{E}rh_{\varkappa-1}^{(2)}(Er)A_{-}, \quad (2.41)$$

$$iP_{\varkappa}^{B_{+,m}} = -i\sqrt{E - 2\omega}rh_{\varkappa}^{(1)}[(E - 2\omega)r]B_{+,m}, \quad Q_{\varkappa}^{B_{+,m}} = \sqrt{E - 2\omega}rh_{\varkappa-1}^{(1)}[(E - 2\omega)r]B_{+,m}, \quad (2.42)$$

$$iP_{\varkappa}^{B_{-,m}} = -i\sqrt{E}rh_{\varkappa}^{(1)}(Er)B_{-,m}, \quad Q_{\varkappa}^{B_{-,m}} = \sqrt{E}rh_{\varkappa-1}^{(1)}(Er)B_{-,m}, \quad (2.43)$$

while these for $-\varkappa < 0$ ($j = \ell - 1$) are

$$iP_{-\varkappa}^{A-} = \sqrt{E}rh_{\varkappa-1}^{(2)}(Er)A_{-}, \quad Q_{-\varkappa}^{A-} = -i\sqrt{E}rh_{\varkappa}^{(2)}(Er)A_{-}, \quad (2.44)$$

$$iP_{-\varkappa}^{B_{+,m}} = \sqrt{E - 2\omega}rh_{\varkappa-1}^{(1)}[(E - 2\omega)r]B_{+,m}, \quad Q_{-\varkappa}^{B_{+,m}} = -i\sqrt{E - 2\omega}rh_{\varkappa}^{(1)}[(E - 2\omega)r]B_{+,m}, \quad (2.45)$$

$$iP_{-\varkappa}^{B_{-,m}} = \sqrt{E}rh_{\varkappa-1}^{(1)}(Er)B_{-,m}, \quad Q_{-\varkappa}^{B_{-,m}} = -i\sqrt{E}rh_{\varkappa}^{(1)}(Er)B_{-,m}. \quad (2.46)$$

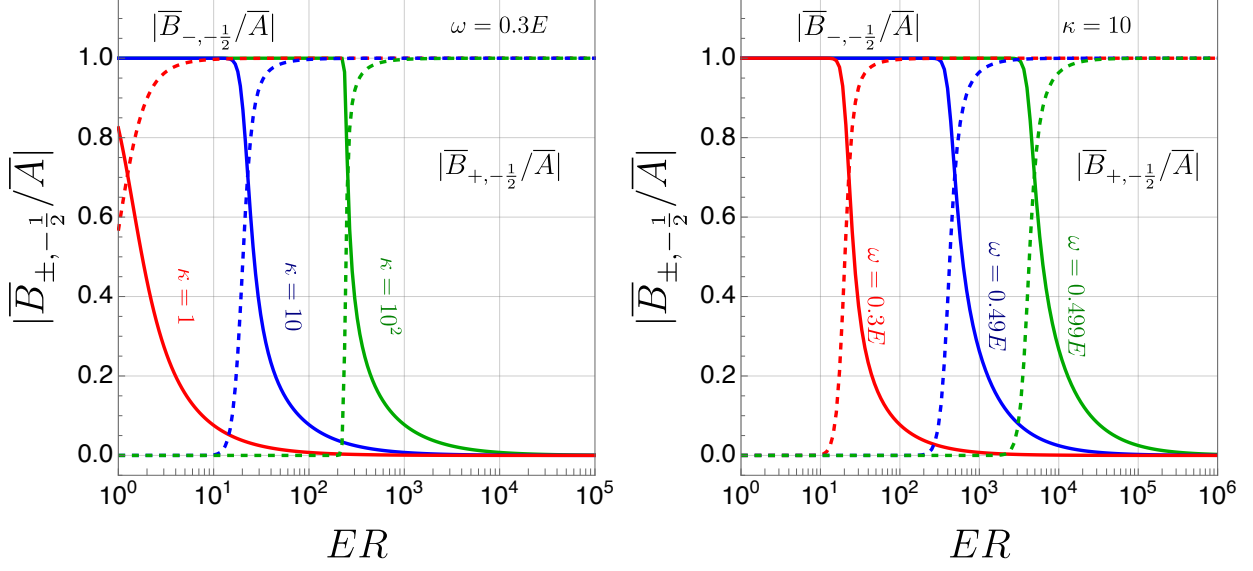


Figure 2: The ER -dependence of the absolute values of the coefficients $\bar{B}_{\pm, -\frac{1}{2}}$ for fixed parameters: fixed $\kappa = 10$ in the right panel, while fixed $\omega/E = 0.3$ in the left panel. $\bar{B}_{-, -\frac{1}{2}}$ is depicted as the solid lines, while $\bar{B}_{+, -\frac{1}{2}}$ is depicted as the dashed lines.

Here, A_- and $B_{\pm, m}$ denote the coefficients for the quark wave functions, not spinors unlike the previous two subsections.

Since we assume that the injected energy E is less than the gluino mass and the field value of the scalar field, the wave function for the heavy fermions is given by a linear combination of the modified spherical Bessel functions. Gluinos mediate outside the Q-ball and are written by the use of spherical Bessel functions if the energy of incoming quark is sufficiently large. The wave function of gluinos should be analytic at $r \rightarrow \infty$ and be described by the second kind of the modified spherical Bessel function $k_n(x)$. Meanwhile, the wave functions for the fermions in the mass basis inside the Q-ball should be analytic at $r \rightarrow 0$, and hence the wave functions are described by the first kind of the modified spherical Bessel function $i_n(x)$. The explicit form of the radial functions for the massive fermions is given in Appendix B.

We find the coefficients after matching the wave functions at the Q-ball boundary. We assume $M_{(\pm)}R \gg \kappa$ and use the asymptotic form of the modified spherical Bessel functions at large $M_{(\pm)}R$. Then, we find the solution for the reflected quark as follows:

$$B_{+, -\frac{1}{2}} = \sqrt{\frac{E}{E - 2\omega}} \frac{h_{\kappa-1}^{(1)}(ER)h_{\kappa}^{(2)}(ER) - h_{\kappa}^{(1)}(ER)h_{\kappa-1}^{(2)}(ER)}{h_{\kappa-1}^{(1)}(ER)h_{\kappa-1}^{(1)}[(E - 2\omega)R] - h_{\kappa}^{(1)}(ER)h_{\kappa}^{(1)}[(E - 2\omega)R]} A_-, \quad (2.47)$$

$$B_{-, -\frac{1}{2}} = -\frac{h_{\kappa-1}^{(2)}(ER)h_{\kappa-1}^{(1)}[(E - 2\omega)R] - h_{\kappa}^{(2)}(ER)h_{\kappa}^{(1)}[(E - 2\omega)R]}{h_{\kappa-1}^{(1)}(ER)h_{\kappa-1}^{(1)}[(E - 2\omega)R] - h_{\kappa}^{(1)}(ER)h_{\kappa}^{(1)}[(E - 2\omega)R]} A_-, \quad (2.48)$$

and $B_{\pm, \frac{1}{2}} = 0$. The coefficients for the massive fermions are listed in Appendix B. We consider the analytical solution in several limits: $ER, (E - 2\omega)R \gg \kappa$, $ER \gg \kappa \gg (E - 2\omega)R$, and $\kappa \gg ER, (E - 2\omega)R$. The asymptotic forms of these coefficients at the leading order of expansion

parameters for each limit are as follows.

$$B_{+,-\frac{1}{2}} = \frac{2i}{[(2\kappa-1)!!]^2} \sqrt{\frac{E-2\omega}{E}} (ER)^\kappa [(E-2\omega)R]^\kappa A_-,$$

$$B_{-,-\frac{1}{2}} = A_-, \quad ER, (E-2\omega)R \ll \kappa, \quad (2.49)$$

$$B_{+,-\frac{1}{2}} = -i^\kappa \sqrt{\frac{E-2\omega}{E}} \frac{[(E-2\omega)R]^\kappa}{(2\kappa-1)!!} \frac{e^{-iER} A_-}{i(2\kappa-1)},$$

$$B_{-,-\frac{1}{2}} = -(-1)^{\kappa+1} e^{-2iER} A_-, \quad (E-2\omega)R \ll \kappa \ll ER, \quad (2.50)$$

$$B_{+,-\frac{1}{2}} = i(-1)^\kappa \sqrt{\frac{E-2\omega}{E}} e^{-2i(E-\omega)R} A_-,$$

$$B_{-,-\frac{1}{2}} = i(-1)^\kappa \frac{2\kappa\omega R}{ER(E-2\omega)R} e^{-2iER} A_-, \quad \kappa \ll ER, (E-2\omega)R. \quad (2.51)$$

An orbital angular momentum for classical scattering is given by the product of the injected energy E and the impact parameter b . When the orbital angular momentum satisfies $ER \ll \ell \simeq \kappa$ (i.e., $R \ll b$), the incoming quark does not collide with the Q-ball. As shown in the asymptotic forms, $B_{+,-\frac{1}{2}}$ is quite suppressed by $(ER)^\kappa$ and $[(E-2\omega)R]^\kappa$ while $B_{-,-\frac{1}{2}}$ is not. Therefore, the final-state quark has a left-handed chirality in the $ER, (E-2\omega)R \ll \kappa$ limit. In the region of $(E-2\omega)R \ll \kappa \ll ER$ (i.e., $b \ll R$), the incoming quark collides with the Q-ball, but this is scattering with a sizable oblique angle. The asymptotic form of $B_{+,-\frac{1}{2}}$ in the region is only suppressed by $[(E-2\omega)R]^\kappa$, and hence the scattering is interpreted as the elastic scattering. Finally, as $\ell \simeq \kappa \ll ER, (E-2\omega)R$, the incoming quark enters almost perpendicular to the Q-ball surface. Contrary to the previous two cases, the asymptotic form of $B_{-,-\frac{1}{2}}$ is only suppressed by κ/ER . Therefore, as we saw in Section 2.1, the reflected quark has a right-handed chirality, namely the incoming quark is reflected as the right-handed anti-quark.

Fig. 2 shows the ER dependence of the absolute value of the coefficients $B_{\pm,-\frac{1}{2}}$. All of coefficients are normalized as $\bar{A}_- \equiv A_-/\sqrt{E}$, $\bar{B}_{+,-\frac{1}{2}} \equiv B_{+,-\frac{1}{2}}/\sqrt{E-2\omega}$, and $\bar{B}_{-,-\frac{1}{2}} \equiv B_{-,-\frac{1}{2}}/\sqrt{E}$. In this figure, we plot $\bar{B}_{+,-\frac{1}{2}}$ as dashed lines and $\bar{B}_{-,-\frac{1}{2}}$ as solid lines. The chemical potential is fixed to be $\omega = 0.3E$ and take $\kappa = 1$ (red), $\kappa = 10$ (blue), and $\kappa = 10^2$ (green) in the left panel. As expected, the constant $\bar{B}_{-,-\frac{1}{2}}$ begins to decay as $ER \simeq \kappa$ and goes to zero at large ER , while the constant $\bar{B}_{+,-\frac{1}{2}}$ begins to develop as $ER \simeq \kappa$ and goes to unity at large ER . The total angular momentum κ is fixed $\kappa = 10$, and we take $\omega = 0.3E$ (red), $\omega = 0.49E$ (blue), and $\omega = 0.499E$ (green) in the right panel. Even if $ER \gtrsim \kappa$, the reflected quark has a left chirality unless the injected energy is sufficiently larger than the chemical potential, namely $(E-2\omega)R \gg \kappa$.

We show the phase of the coefficients $B_{\pm,-\frac{1}{2}}$ with fixed κ in Fig. 3. There, we take the ratio of the coefficients with κ and $\kappa-1$ to remove the common phases, which approach to $e^{-i(E-\omega)R}$ and e^{-iER} in the large $ER, (E-2\omega)R$ limits. We note that we add the subscript κ in $B_{\kappa,\pm,-\frac{1}{2}}$ to show κ -dependence explicitly. As shown in the asymptotic forms, the ratio of the coefficients $B_{\kappa,-,-\frac{1}{2}}/B_{\kappa-1,-,-\frac{1}{2}}$ approximately goes to (-1) as $ER \gg \kappa$ even for small $(E-2\omega)R$. Meanwhile, the ratio $B_{\kappa,+,-\frac{1}{2}}/B_{\kappa-1,+,-\frac{1}{2}}$ approaches to i in the region $ER \gg \kappa \gg (E-2\omega)R$, and then approximately goes to (-1) as $ER(E-2\omega)R \gg \kappa$. Therefore, as shown in the figure, the relative phase goes to $\pi/2$ as $ER > \kappa$ as expected from the hard sphere scattering (see Ref. [26]), and then it approaches to π for $(E-2\omega)R > \kappa$.

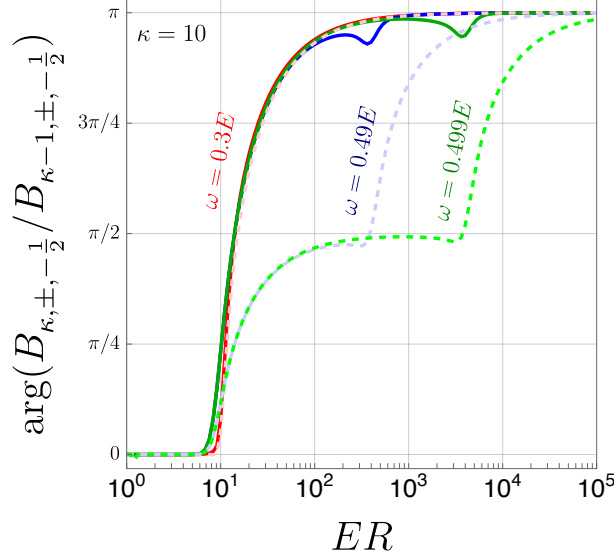


Figure 3: The relative phase of the coefficients $B_{\pm, -\frac{1}{2}}$ with fixed $\kappa = 10$. $B_{-, -\frac{1}{2}}$ is depicted as the solid lines with the same color code as Fig. 2, while $B_{+, -\frac{1}{2}}$ is depicted as the dashed lines with light colors.

As with the previous subsection, we consider the S -matrix for the scattering with $\omega = 0$. For given κ (in other words, the total angular momentum j), the S -matrix for the Q-ball scattering with quark is block-diagonalized with respect to the mass eigenstates:

$$S'^{\kappa} = \begin{pmatrix} \mathbf{1}_2 & 0 \\ 0 & S_2^{\kappa} \end{pmatrix}. \quad (2.52)$$

Here, the upper block corresponds to the scattering of the massless fermion inside the Q-ball, while the lower block corresponds to that of the massive fermion. The in-state for each block is labelled by the helicity, so each is 2×2 sub-matrix. For the positive κ (in other words, $\ell = j + 1/2$), the sub-matrix is

$$S_2^{\kappa} = (-1)^{\kappa} i e^{2iER} \begin{pmatrix} 0 & 1 \\ 1 & 0 \end{pmatrix}, \quad (2.53)$$

while for the negative $-\kappa$ (in other words, $\ell = j - 1/2$), the sub-matrix is

$$S_2^{-\kappa} = (-1)^{-\kappa-1} i e^{2iER} \begin{pmatrix} 0 & 1 \\ 1 & 0 \end{pmatrix}. \quad (2.54)$$

Similarly to the previous case, we can write the S -matrix in terms of the interaction basis of quarks outside the Q-ball by the field rotation.

$$S^{\kappa} = \begin{pmatrix} \sin^2 \alpha \mathbf{1}_2 + \cos^2 \alpha S_2^{\kappa} & \cos \alpha \sin \alpha (\mathbf{1}_2 - S_2^{\kappa}) \\ \cos \alpha \sin \alpha (\mathbf{1}_2 - S_2^{\kappa}) & \cos^2 \alpha \mathbf{1}_2 + \sin^2 \alpha S_2^{\kappa} \end{pmatrix}. \quad (2.55)$$

Again, this indicates that the incident quark can be reflected as not only its anti-quark but also the anti-quark of another species.

3 Implication to Nucleon Scattering with Q-ball

In this section, we discuss the implication to the nucleon scattering with the Q-ball from the observation in the last section. We naively expect that the incoming nucleon is reflected as nucleon, pions, or anti-nucleon. However, due to the energy cost by the chemical potential, it is challenging to be reflected as anti-nucleon in gravitationally bounded halos such as our Milky-Way. The Q-ball DM scatters off the nucleon with a typical velocity of $v \sim 10^{-3}$, and hence the kinetic energy of the nucleon in the Q-ball rest frame is

$$E_{\text{kin}} = \frac{1}{2} m_N v^2 \simeq 0.47 \text{ keV} \left(\frac{v}{10^{-3}} \right)^2. \quad (3.1)$$

Meanwhile, the energy cost ω is inversely proportional to the Q-ball radius [1, 6, 27, 28] and is numerically given by

$$\omega \simeq R^{-1} \simeq 20 \text{ MeV} \left(\frac{10 \text{ fm}}{R} \right). \quad (3.2)$$

As shown in the previous section, the nucleon can be reflected as the anti-nucleon only when the scattering process can pay the energy cost $3 \times 2\omega$. It is impossible to emit the anti-nucleon due to the energy cost. Meanwhile, it would be possible that a constituent quark inside nucleon is reflected as an anti-quark since it has a momentum of $\Lambda_{\text{QCD}} \simeq 200 \text{ MeV}$, which can be larger than the energy cost 2ω . Due to the linear potential by the strong interaction, the single anti-quark emission is prohibited. This process can be interpreted as the nucleon absorption with the pion emission. In this case, the Q-ball is in an excited state, which can decay into the stable configuration after emitting a nucleon or pions. Since our treatment does not incorporate such a back-reaction process, it is beyond the scope of this work.

Other channels for the nucleon scattering, with conversion into pions or a nucleon, would charge up and down the Q-ball. Once the Q-ball is negatively charged, the Coulomb interaction between proton and Q-ball is attractive, and the charged Q-ball scatters with protons until the Q-ball is positively charged. Let assume that the Q-ball has the radius R and the electromagnetic (positive) charge Z_Q . The maximal charge of the Q-ball that can scatter with proton is classically determined when the Coulomb potential equals to the kinetic energy of proton. Then, we find the maximal charge of the Q-ball:

$$Z_Q \simeq \frac{m_N R}{2\alpha} v^2 \simeq 0.3 \left(\frac{R}{10^3 \text{ fm}} \right) \left(\frac{v}{10^{-3}} \right)^2. \quad (3.3)$$

Here, m_N is the nucleon mass, $\alpha^{-1} \simeq 137$ is the fine structure constant, and v denotes the relative velocity of the nucleon and the Q-ball. Even if the charge is larger than the maximal value, the Q-ball scatters with the proton via the tunneling, and the scattering cross section between the proton and the Q-ball is suppressed by the Coulomb barrier. The scattering wave function is estimated by the WKB approximation in this case. In the limit of the small DM velocity limit, the Coulomb barrier factor for the wave function is approximately given by

$$\exp \left[- \int_R^{R_2} dr \sqrt{2m_N \left(\frac{Z_Q \alpha}{r} - \frac{Z_Q \alpha}{R_2} \right)} \right] \simeq \exp \left[- \frac{\pi Z_Q \alpha}{v} \left(1 - \frac{4}{\pi} \sqrt{\frac{R}{R_2}} \right) \right]. \quad (3.4)$$

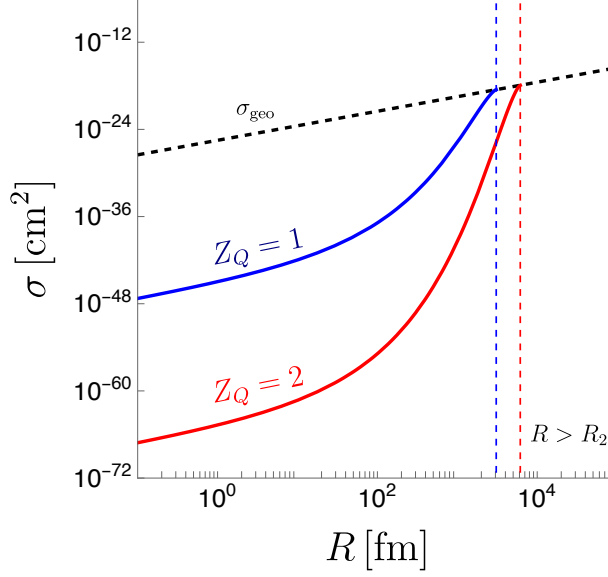


Figure 4: The proton-charged Q-ball scattering cross section. The relative velocity of the Q-ball and the proton is assumed to be $v \simeq 10^{-3}$. The electromagnetic charge of the Q-ball Z_Q is fixed for each solid lines: $Z_Q = 1$ (blue) and $Z_Q = 2$ (red). The thin-dashed vertical lines show the point where $R = R_2$ for each Z_Q with the same color code as the solid lines. The geometric cross section $\sigma_{\text{geo}} = \pi R^2$ is depicted as the black dashed line. The radius R of our interest is $10 \text{ fm} \lesssim R \lesssim \mathcal{O}(1) \text{ nm}$ [1].

Here, $R_2 > R$ denotes the point where the kinetic energy equals to the potential energy,

$$R_2 = \frac{2Z_Q\alpha}{m_N v^2} \simeq 3.07 Z_Q \text{ pm} \left(\frac{10^{-3}}{v} \right)^2. \quad (3.5)$$

The Coulomb barrier suppresses the scattering cross section as far as the Q-ball radius satisfies $R \lesssim R_2$. The scattering cross section consists of the geometric one and the Coulomb barrier factor, and we find

$$\begin{aligned} \sigma &\simeq \pi R^2 \exp \left[-\frac{2\pi Z_Q \alpha}{v} \left(1 - \frac{4}{\pi} \sqrt{\frac{R}{R_2}} \right) \right] \\ &\simeq 3 \times 10^{-24} \text{ cm}^2 \left(\frac{R}{10 \text{ fm}} \right)^2 (1.2 \times 10^{-20})^{Z_Q}. \end{aligned} \quad (3.6)$$

We assume the R/R_2 correction is negligible in order to obtain the last numerical expression.

Fig. 4 depicts the radius R dependence of the scattering cross section for fixed the electromagnetic charge of the Q-ball Z_Q . We assume the relative velocity of the Q-ball and the proton to be $v \simeq 10^{-3}$. The scattering cross section is quite suppressed with the Coulomb barrier factor of $\sim 10^{-20Z_Q}$ at small R . The Coulomb barrier starts to change by an order of magnitude around $R \simeq 10^{-4} R_2$, and then the cross section approaches to the geometric one (shown as the black-dashed line) as R gets larger and the barrier disappears at $R = R_2$.

The discussion of the electromagnetic charge of Q-ball also depends on the corresponding flat direction: we focus on the *udd* flat direction so far. One may consider the Q-balls associated with

other flat directions, such as with $uude$ and $qqq\ell$ which carry not only the baryon number but also the lepton number [7, 8]. For such a case, the Q-ball configuration is stable only when the chemical potential is less than lepton mass (m_e for the $uude$ Q-ball, while neutrino mass for the $qqq\ell$ Q-ball). When we consider the $uude$ ($qqq\ell$) flat direction, the Q-ball scattering with the electron would make the positively-charged Q-ball discharged by converting $e^- \rightarrow e^+$. Thus, if the injected energy satisfies $E > 2\omega$ for the electron scattering, the charged Q-ball is easily discharged. It would also be possible that the injected proton is reflected as the positron.

The charged Q-ball can also be discharged by forming the bound state with the free electrons. The bound state formation cross section at large $\eta = Z_Q\alpha/v$ limit is approximately given by (see Ref. [29] for example)

$$\sigma_{\text{BSF}} \simeq \frac{32\pi}{3\sqrt{3}} \frac{\eta^4 \alpha^3 a_B^2}{n(\eta^2 + n^2)} \simeq 1.1 \times 10^4 \text{ barn} \left(\frac{10^{-3}}{v} \right)^2, \quad (\eta \gg n), \quad (3.7)$$

$$\simeq 6.0 \times 10^4 \text{ barn} \left(\frac{10^{-3}}{v} \right)^4, \quad (\eta \ll n). \quad (3.8)$$

Here, $a_B = Z_Q/m_e\alpha$ is the Bohr radius. The typical radius for this system (with the principal quantum number n) is given by

$$r_c(n) = \frac{n^2}{m_e\alpha Z_Q} \simeq 52.9 \frac{n^2}{Z_Q} \text{ pm}, \quad (3.9)$$

and hence the typical radius can be inside R_2 when

$$Z_Q > 4.15n \left(\frac{v}{10^{-3}} \right). \quad (3.10)$$

For such a case, the electromagnetic force is screened for $r > r_c(n)$, and the Coulomb barrier factor is modified as follows.

$$\exp \left[- \int_R^{r_c(n)} dr \sqrt{2m_N \left(\frac{Z_Q\alpha}{r} - \frac{Z_Q\alpha}{R_2} \right)} \right]. \quad (3.11)$$

Similarly to Fig. 4, it leads to a huge suppression of the scattering cross section by the Coulomb barrier unless the Q-ball radius R approaches to $r_c(n)$.

4 Conclusion and Discussion

It is important to understand the interactions between the Q-ball DM and matters, in order to investigate the experimental signals from the Q-ball DM [20], e.g., in paleo detectors [19]. We have clarified the scattering of the Q-ball DM and quarks with taking into account the chemical potential ω , which is overlooked in the literature. The incoming quark is reflected as the anti-quark when the injected energy of the incoming quark exceeds the energy cost for increasing the baryon number of the Q-ball, 2ω . As for the scattering between the Q-ball DM with the radius of $\mathcal{O}(1)$ fm and the nucleons in our Galaxy (namely, with relative speed of $v \sim 10^{-3}$), the nucleon is not reflected as the anti-nucleon due to the energy cost.

The Q-ball DM can be electromagnetically charged if the energetic proton has scattered with the Q-ball in our Galaxy and if the nucleon scattering with Q-ball would emit nucleon or pions. Once the Q-ball is charged, the scattering cross section to proton is quite suppressed by the Coulomb barrier and the experimental signals are different from the neutral Q-ball [20]. It is worthwhile to clarify what ratio of the Q-ball is electromagnetically charged in our Milky Way by taking into account the dependence on the flat directions.

Acknowledgements

A. K. thanks Kohta Murase and Shigenobu Hirose for encouraging us to work on this study, and also Alexander Kusenko for sharing comments on the draft. A. K. acknowledges partial support from Norwegian Financial Mechanism for years 2014-2021, grant nr 2019/34/H/ST2/00707; and from National Science Centre, Poland, grant DEC-2018/31/B/ST2/02283. The work of T. K. is supported in part by the National Science Foundation of China under Grant Nos. 11675002, 11635001, 11725520, 12235001, and 12250410248.

A Useful Formulae

In this appendix, we summarize the useful formulae for our study.

A.1 Formulae for Analytically-continued momentum

The square root of the matrices $\sigma \cdot k$ and $\bar{\sigma} \cdot k$ with the four-momentum $k = (E, \mathbf{k})$ (the mass $m^2 = E^2 - \mathbf{k}^2$) is expanded as follows.

$$\begin{aligned}\sqrt{\sigma \cdot k} &= \frac{1}{\sqrt{2}} \left(\sqrt{E+m} \mathbb{1} - \frac{1}{\sqrt{E+m}} \mathbf{k} \cdot \boldsymbol{\sigma} \right), \\ \sqrt{\bar{\sigma} \cdot k} &= \frac{1}{\sqrt{2}} \left(\sqrt{E+m} \mathbb{1} + \frac{1}{\sqrt{E+m}} \mathbf{k} \cdot \boldsymbol{\sigma} \right).\end{aligned}\tag{A.1}$$

It is straightforward to extend this formula for the analytically continued momentum in this form. In particular, we just replace the three-momentum $\mathbf{k} \rightarrow i\boldsymbol{\kappa}$ with a real vector $\boldsymbol{\kappa}$ as $E < m$. The complex conjugate of the matrix is

$$\sigma^2 \left(\sqrt{\sigma \cdot k^*} \right)^* \sigma^2 = \sqrt{\bar{\sigma} \cdot k}.\tag{A.2}$$

Using this equality, the complex conjugate of the negative-frequency part of the wave function in Eq. (2.13) is calculated as follows.

$$\left[\sqrt{\sigma \cdot p^*} (-i\sigma_2) A^* e^{ip^*x} \right]^* = (-i\sigma_2) \sqrt{\bar{\sigma} \cdot p} A e^{-ipx},\tag{A.3}$$

A.2 Spinor Spherical Harmonics

We construct the spherical-wave solutions of the Dirac equation, which are important for describing out-going states of the scattering of the Dirac fermion (see [30–32]). Now, we consider a state of the

total angular momentum $\mathbf{J} = \mathbf{L} + \mathbf{S}$ with the orbital angular momentum operator \mathbf{L} and the spin operator \mathbf{S} . The state of the total angular momentum is a simultaneous eigenstate of J^2 , J_z , L^2 , and S^2 (with the eigenvalues of $j(j+1)$, m , $\ell(\ell+1)$, and $s(s+1)$, respectively), and we denote the eigenstate as $|j, m; \ell, s\rangle$. The state of the total angular momentum is given by the linear combination of the direct product of the states of \mathbf{L} and \mathbf{S} .

$$|j, m; \ell, s\rangle = \sum_{m_s} C(\ell, s, j; m_\ell, m_s, m) |\ell, m_\ell\rangle |s, m_s\rangle. \quad (\text{A.4})$$

Here, $C(\ell, s, j; m_\ell, m_s, m)$ is the Clebsch-Gordan coefficient (CGC), and $m = m_\ell + m_s$.

Now, we consider the state with the spin-1/2 and the orbital angular momentum ℓ . The total angular momentum is given by $j = \ell \pm 1/2$. For fixed j and m , we have two independent CGCs.

$$x = C(\ell, 1/2, j; m - 1/2, 1/2, m), \quad y = C(\ell, 1/2, j; m + 1/2, -1/2, m). \quad (\text{A.5})$$

Using these coefficients, we write the state as

$$\left| j, m; \ell, \frac{1}{2} \right\rangle = x \left| \ell, m - \frac{1}{2} \right\rangle \left| \frac{1}{2}, \frac{1}{2} \right\rangle + y \left| \ell, m + \frac{1}{2} \right\rangle \left| \frac{1}{2}, -\frac{1}{2} \right\rangle. \quad (\text{A.6})$$

The orthogonality relation $\langle j', m'; \ell', 1/2 | j, m; \ell, 1/2 \rangle = \delta_{j',j} \delta_{m',m}$ gives $x^2 + y^2 = 1$. The state $|j, m; \ell, 1/2\rangle$ is the eigenstate of the spin-orbit coupling $\Lambda = 2\mathbf{L} \cdot \mathbf{S} = \mathbf{J}^2 - \mathbf{L}^2 - \mathbf{S}^2$.

$$\Lambda \left| j, m; \ell, \frac{1}{2} \right\rangle = \lambda \left| j, m; \ell, \frac{1}{2} \right\rangle, \quad (\text{A.7})$$

with the eigenvalue $\lambda = \ell$ ($j = \ell + 1/2$) or $\lambda = -\ell - 1$ ($j = \ell - 1/2$). Meanwhile, acting $\Lambda = 2\mathbf{L} \cdot \mathbf{S} = 2L_z S_z + L_+ S_- + L_- S_+$ on the right-hand side of Eq. (A.6), we have two independent equations that are obtained from coefficients of each state, $|\ell, m - 1/2\rangle |1/2, 1/2\rangle$ and $|\ell, m + 1/2\rangle |1/2, -1/2\rangle$.

$$\lambda x = \left(m - \frac{1}{2} \right) x + \sqrt{\left(\ell - m + \frac{1}{2} \right) \left(\ell + m + \frac{1}{2} \right)} y, \quad (\text{A.8})$$

$$\lambda y = \sqrt{\left(\ell - m + \frac{1}{2} \right) \left(\ell + m + \frac{1}{2} \right)} x - \left(m + \frac{1}{2} \right) y, \quad (\text{A.9})$$

and we find the ratio y/x to be

$$\frac{y}{x} = \frac{\lambda - m + \frac{1}{2}}{\sqrt{\left(\ell - m + \frac{1}{2} \right) \left(\ell + m + \frac{1}{2} \right)}}. \quad (\text{A.10})$$

We take a sign convention, $y > 0$. Combining them, we obtain the CGCs for the spin and the orbital angular momentum as shown in Table 1.

The spherical spinor $\Omega_{j\ell m}$ is an eigenfunction of the total angular momentum \mathbf{J}^2 and J_z . $\Omega_{j,\ell,m}$ is given by a combination of the spherical harmonics $Y_{\ell,m}$, the eigenfunction of the orbital angular

Table 1: List of the Clebsch-Gordan coefficients for $\mathbf{L} + \mathbf{S}$.

	$j = \ell + 1/2$	$j = \ell - 1/2$
$m_s = 1/2$	$\sqrt{\frac{\ell + m + \frac{1}{2}}{2\ell + 1}}$	$-\sqrt{\frac{\ell - m + \frac{1}{2}}{2\ell + 1}}$
$m_s = -1/2$	$\sqrt{\frac{\ell - m + \frac{1}{2}}{2\ell + 1}}$	$\sqrt{\frac{\ell + m + \frac{1}{2}}{2\ell + 1}}$

momentum, and the two-component spinor χ_m . In other words, the spherical spinor is given by the projection of a state onto the angle coordinate and the spinor space.

$$\begin{aligned}
\Omega_{j,\ell,m}(\theta, \phi) &= \langle \theta, \phi; \chi | j, m; \ell, 1/2 \rangle \\
&= \sum_{m_s} C(\ell, 1/2, j; m - m_s, m_s, m) \langle \theta, \phi | \ell, m - m_s \rangle \langle \chi | s, m_s \rangle \\
&= \sum_{m_s} C(\ell, 1/2, j; m - m_s, m_s, m) Y_{\ell, m - m_s}(\theta, \phi) \chi_{m_s}.
\end{aligned} \tag{A.11}$$

Here, the two-component spinor are given by

$$\chi_{\frac{1}{2}} = \begin{pmatrix} 1 \\ 0 \end{pmatrix}, \quad \chi_{-\frac{1}{2}} = \begin{pmatrix} 0 \\ 1 \end{pmatrix}. \tag{A.12}$$

The CGCs for the spin-1/2 and the orbital angular momentum ℓ is given by Table 1, and hence we have explicit forms of the spherical spinors as follows.

$$\begin{aligned}
\Omega_{\ell+\frac{1}{2},\ell,m}(\theta, \phi) &= \begin{pmatrix} \sqrt{\frac{\ell+m+1/2}{2\ell+1}} Y_{\ell, m-\frac{1}{2}}(\theta, \phi) \\ \sqrt{\frac{\ell-m+1/2}{2\ell+1}} Y_{\ell, m+\frac{1}{2}}(\theta, \phi) \end{pmatrix}, \\
\Omega_{\ell-\frac{1}{2},\ell,m}(\theta, \phi) &= \begin{pmatrix} -\sqrt{\frac{\ell-m+1/2}{2\ell+1}} Y_{\ell, m-\frac{1}{2}}(\theta, \phi) \\ \sqrt{\frac{\ell+m+1/2}{2\ell+1}} Y_{\ell, m+\frac{1}{2}}(\theta, \phi) \end{pmatrix}.
\end{aligned} \tag{A.13}$$

Now, we recall properties of the spherical harmonics $Y_{\ell,m}$. The spherical harmonics is written with the associated Legendre functions P_ℓ^m as follows.

$$\begin{aligned}
Y_{\ell,m}(\theta, \phi) &= \sqrt{\frac{2\ell+1}{4\pi} \frac{(\ell-m)!}{(\ell+m)!}} e^{im\phi} P_\ell^{|m|}(\cos \theta), \\
P_\ell^{|m|}(x) &= \frac{(-1)^{|m|}}{2^\ell \ell!} (1-x^2)^{|m|/2} \frac{d^{\ell+|m|}}{dx^{\ell+|m|}} (x^2-1)^\ell.
\end{aligned} \tag{A.14}$$

We choose the phase convention as in the above equation. The normalization of the spherical harmonics is chosen so that the orthogonal relation is given by

$$\int d\cos\theta d\phi Y_{\ell'm'}^*(\theta, \phi) Y_{\ell m}(\theta, \phi) = \delta_{\ell',\ell} \delta_{m',m}. \tag{A.15}$$

Under the parity transformation, $\mathbf{r} \rightarrow -\mathbf{r}$ (in terms of angles, $\{\theta, \phi\} \rightarrow \{\pi - \theta, \phi + \pi\}$), the spherical harmonics changes only by a sign factor.

$$PY_{\ell,m}(\theta, \phi) = Y_{\ell,m}(\pi - \theta, \phi + \pi) = (-1)^\ell Y_{\ell,m}(\theta, \phi). \quad (\text{A.16})$$

Since the state $|j, m; \ell, s\rangle$ is an eigenstate of the spin-orbit coupling, the spherical spinors are also the eigenfunctions of the coupling. Conventionally, the spherical spinors are labelled by the eigenvalues κ of an operator $K = -1 - 2\mathbf{L} \cdot \mathbf{S}$. The operation of K on the spherical spinors is given by

$$K\Omega_{j,\ell,m}(\theta, \phi) = \kappa\Omega_{j,\ell,m}(\theta, \phi). \quad (\text{A.17})$$

Here, $\kappa = -1 - \ell$ for $j = \ell + 1/2$, and $\kappa = \ell$ for $j = \ell - 1/2$. In other words, $\kappa = \mp(j + 1/2)$ for $j = \ell \pm 1/2$. The absolute value of κ determines j , and the sign of κ determines the relative sign of $j - \ell$. Hence, a compact notation for the spherical spinors, labelled by κ , is often used.

$$\Omega_{\kappa,m}(\theta, \phi) = \Omega_{j,\ell,m}(\theta, \phi). \quad (\text{A.18})$$

Let us now discuss the properties of the spherical spinors. The orthogonal relation of the spherical spinors follows from that of the spherical harmonics $Y_{\ell,m}$ and is given by

$$\int d\cos\theta d\phi \Omega_{\kappa',m'}^\dagger \Omega_{\kappa,m} = \delta_{\kappa',\kappa} \delta_{m',m}. \quad (\text{A.19})$$

The parity transformation of the spherical spinors also follows from that of the spherical harmonics as follows.

$$P\Omega_{\kappa,m}(\theta, \phi) = (-1)^\ell \Omega_{\kappa,m}(\theta, \phi). \quad (\text{A.20})$$

Since $\ell = j \pm 1/2$, the sign factor differs only by (-1) for fixed j with different sign of κ . Therefore, the spherical spinors have opposite parities for κ and $-\kappa$.

Let us consider operations $\boldsymbol{\sigma} \cdot \hat{\mathbf{r}}$ with $\hat{\mathbf{r}} = \mathbf{r}/r$ and $\boldsymbol{\sigma} \cdot \mathbf{p}$ on the spherical spinors for constructing the solution of the Dirac equation. The parity operator changes the sign of $\boldsymbol{\sigma} \cdot \hat{\mathbf{r}}$. Therefore, the operation of $\boldsymbol{\sigma} \cdot \hat{\mathbf{r}}$ on $\Omega_{\kappa,m}$ is proportional to $\Omega_{-\kappa,m}$,

$$\boldsymbol{\sigma} \cdot \hat{\mathbf{r}} \Omega_{\kappa,m}(\theta, \phi) = a \Omega_{-\kappa,m}(\theta, \phi). \quad (\text{A.21})$$

Here, a is a constant satisfying $a^2 = 1$ because of an identity $(\boldsymbol{\sigma} \cdot \hat{\mathbf{r}})(\boldsymbol{\sigma} \cdot \hat{\mathbf{r}}) = 1$. We evaluate both sides of the above equation with $\theta = 0$, and one can establish $a = -1$ independent of the sign of κ . Using the identity $(\boldsymbol{\sigma} \cdot \hat{\mathbf{r}})(\boldsymbol{\sigma} \cdot \hat{\mathbf{r}}) = 1$, one can rewrite $\boldsymbol{\sigma} \cdot \mathbf{p}$ as follows.

$$\boldsymbol{\sigma} \cdot \mathbf{p} = (\boldsymbol{\sigma} \cdot \hat{\mathbf{r}}) \left(\hat{\mathbf{r}} \cdot \mathbf{p} + i \frac{\boldsymbol{\sigma} \cdot \mathbf{L}}{r} \right). \quad (\text{A.22})$$

We can use the identity $\boldsymbol{\sigma} \cdot \mathbf{L} = -1 - K$ for simplifying the second term in the bracket. Assuming the function $f(r)$ depending only on the radius coordinate r , the operation on a function $f(r)\Omega_{\kappa m}(\theta, \phi)$ is given by

$$\boldsymbol{\sigma} \cdot \mathbf{p} [f(r)\Omega_{\kappa m}(\theta, \phi)] = i \left[\frac{df}{dr} + \frac{1 + \kappa}{r} f(r) \right] \Omega_{-\kappa m}(\theta, \phi). \quad (\text{A.23})$$

We are now ready for discussing the solution of the Dirac equation with the spherically symmetric (central force) potential $V(r)$. The four-component Dirac spinor Ψ satisfies the time-independent Dirac equation:

$$H_D \Psi = E \Psi, \quad H_D = \boldsymbol{\alpha} \cdot \mathbf{p} + \beta M + V(r), \quad (\text{A.24})$$

where H_D is the Dirac Hamiltonian, M denotes the mass of the Dirac fermion, and E denotes the energy. $\boldsymbol{\alpha}$ and β correspond to the 4×4 Dirac matrices in the Dirac basis³:

$$\boldsymbol{\alpha} = \begin{pmatrix} 0 & \boldsymbol{\sigma} \\ \boldsymbol{\sigma} & 0 \end{pmatrix}, \quad \beta = \begin{pmatrix} \mathbb{1} & 0 \\ 0 & -\mathbb{1} \end{pmatrix}, \quad (\text{A.29})$$

and we note that the γ_5 -matrix in the Dirac basis is

$$\gamma_5 = \begin{pmatrix} 0 & \mathbb{1} \\ \mathbb{1} & 0 \end{pmatrix}. \quad (\text{A.30})$$

When the potential is spherically symmetric, the total angular momentum $\mathbf{J} = \mathbf{L} + \mathbf{S}$ commutes with the Dirac Hamiltonian. The solution is the simultaneous eigenstate of the energy and the total angular momentum J^2 and J_z . As mentioned above, the eigenfunction for the total angular momentum J^2 and J_z is given by the spherical spinors. We have two spherical spinors $\Omega_{\kappa,m}$ and $\Omega_{-\kappa,m}$ for given j , but they have opposite parity. The wave function is decomposed into the radial part and two spherical spinors:

$$\Psi_{\kappa,m}(\mathbf{r}) = \frac{1}{r} \begin{pmatrix} iP_{\kappa}(r)\Omega_{\kappa,m}(\theta, \phi) \\ Q_{\kappa}(r)\Omega_{-\kappa,m}(\theta, \phi) \end{pmatrix}. \quad (\text{A.31})$$

We label the wave function the quantum numbers (κ, m) instead of (j, ℓ, m) . We note again that the absolute value of κ determines the size of j and the sign of κ determines $j - \ell$. Using Eq. (A.23),

³The notation for γ in the Dirac basis is given by

$$\gamma_D^0 = \beta = \begin{pmatrix} \mathbb{1} & 0 \\ 0 & -\mathbb{1} \end{pmatrix}, \quad \gamma_D = \beta \boldsymbol{\alpha} = \begin{pmatrix} 0 & \boldsymbol{\sigma} \\ -\boldsymbol{\sigma} & 0 \end{pmatrix}. \quad (\text{A.25})$$

They are related with those in the Weyl basis as

$$\gamma_W^0 = U \gamma_D^0 U^\dagger = \begin{pmatrix} 0 & \mathbb{1} \\ \mathbb{1} & 0 \end{pmatrix}, \quad \gamma_W = U \gamma_D U^\dagger = \begin{pmatrix} 0 & \boldsymbol{\sigma} \\ -\boldsymbol{\sigma} & 0 \end{pmatrix}, \quad \gamma_{5W} = U \gamma_{5D} U^\dagger = \begin{pmatrix} -\mathbb{1} & 0 \\ 0 & \mathbb{1} \end{pmatrix}, \quad (\text{A.26})$$

with the rotation matrix

$$U = \frac{1}{\sqrt{2}} \begin{pmatrix} \mathbb{1} & -\mathbb{1} \\ \mathbb{1} & \mathbb{1} \end{pmatrix}. \quad (\text{A.27})$$

The spinors in the Weyl basis are

$$\begin{aligned} u_W(\mathbf{p}, \chi) &= U u_D(\mathbf{p}, \chi) = \begin{pmatrix} \sqrt{\boldsymbol{\sigma} \cdot \mathbf{k}} \chi \\ \sqrt{\boldsymbol{\sigma} \cdot \mathbf{k}} \chi \end{pmatrix}, \\ v_W(\mathbf{p}, \chi) &= U v_D(\mathbf{p}, \chi) = \begin{pmatrix} -\sqrt{\boldsymbol{\sigma} \cdot \mathbf{k}} \chi \\ \sqrt{\boldsymbol{\sigma} \cdot \mathbf{k}} \chi \end{pmatrix}. \end{aligned} \quad (\text{A.28})$$

one obtains the coupled first-order differential equations for the radial functions $P_\kappa(r)$ and $Q_\kappa(r)$.

$$\begin{aligned} [V(r) + M]P_\kappa + \left(\frac{d}{dr} - \frac{\kappa}{r}\right)Q_\kappa &= EP_\kappa, \\ -\left(\frac{d}{dr} + \frac{\kappa}{r}\right)P_\kappa + [V(r) - M]Q_\kappa &= EQ_\kappa. \end{aligned} \quad (\text{A.32})$$

In order to consider the scattering of fermions under the spherical potential, we first expand the plane-wave Dirac wave functions in terms of the spherical spinors. The plane-wave solutions of Eq. (A.24) (with $V = 0$) are

$$\begin{aligned} \Psi(\mathbf{r}, t, \chi) &= u(\mathbf{p}, \chi)e^{-iEt+i\mathbf{p}\cdot\mathbf{r}}, & u(\mathbf{p}, \chi) &= \sqrt{E+M} \begin{pmatrix} \chi \\ \frac{\boldsymbol{\sigma}\cdot\mathbf{p}}{E+M}\chi \end{pmatrix}, \\ \Psi(\mathbf{r}, t, \chi) &= v(\mathbf{p}, \chi)e^{iEt-i\mathbf{p}\cdot\mathbf{r}}, & v(\mathbf{p}, \chi) &= \sqrt{E+M} \begin{pmatrix} \frac{\boldsymbol{\sigma}\cdot\mathbf{p}}{E+M}\chi \\ \chi \end{pmatrix}. \end{aligned} \quad (\text{A.33})$$

Here, we take the normalization of the Dirac spinors as

$$\bar{u}(\mathbf{p}, \chi')u(\mathbf{p}, \chi) = 2M\chi'^\dagger\chi, \quad \bar{v}(\mathbf{p}, \chi')v(\mathbf{p}, \chi) = -2M\chi'^\dagger\chi. \quad (\text{A.34})$$

The Dirac equation for the radial functions (A.32) is rewritten as the second-order differential equations under the assumption of $V = 0$. Fixed $p^2 = E^2 - M^2$, one easily finds the solutions that are analytic at $pr \rightarrow 0$. The solution is given by

$$\begin{aligned} P_\varkappa(r) &= Arj_\varkappa(pr), & Q_\varkappa(r) &= Brj_{\varkappa-1}(pr), \\ P_{-\varkappa}(r) &= Arj_{-\varkappa-1}(pr), & Q_{-\varkappa}(r) &= Brj_{-\varkappa}(pr). \end{aligned} \quad (\text{A.35})$$

Here, A and B are constants, and $\varkappa > 0$. Inserting these solutions to the coupled Dirac equations, Eq. (A.32), for the positive energy solution, one finds

$$B = \mp \frac{p}{E+M}A, \quad (\kappa \gtrless 0). \quad (\text{A.36})$$

For the negative energy solution, what we have to do is to replace $E \rightarrow -E$. Instead, to match the plane-wave solution with negative energy, we use the following convention:

$$A = \pm \frac{p}{E+M}B, \quad (\kappa \gtrless 0). \quad (\text{A.37})$$

The overall normalization is adjusted to the normalization of the plane-wave solution. The spherical-wave solutions for the positive energy and for the negative energy are

$$\Psi_{\kappa,m}(\mathbf{r}, t, \chi) = u_{\kappa,m}(\mathbf{r}, \mathbf{p}, \chi)e^{-iEt}, \quad \Psi_{\kappa,m}(\mathbf{r}, t, \chi) = v_{\kappa,m}(\mathbf{r}, \mathbf{p}, \chi)e^{iEt}. \quad (\text{A.38})$$

with the Dirac spinors for the spherical-wave solutions:

$$u_{\varkappa,m}(\mathbf{r}, p) = \sqrt{4\pi(E+M)} \begin{pmatrix} -ij_{j+\frac{1}{2}}(pr)\Omega_{j,j+\frac{1}{2},m}(\theta, \phi) \\ \frac{p}{E+M}j_{j-\frac{1}{2}}(pr)\Omega_{j,j-\frac{1}{2},m}(\theta, \phi) \end{pmatrix}, \quad (\text{A.39})$$

$$u_{-\varkappa,m}(\mathbf{r}, p) = \sqrt{4\pi(E+M)} \begin{pmatrix} j_{j-\frac{1}{2}}(pr)\Omega_{j,j-\frac{1}{2},m}(\theta, \phi) \\ -i\frac{p}{E+M}j_{j+\frac{1}{2}}(pr)\Omega_{j,j+\frac{1}{2},m}(\theta, \phi) \end{pmatrix}, \quad (\text{A.40})$$

for the positive energy (with positive \varkappa), and with

$$v_{\varkappa,m}(\mathbf{r}, p) = \sqrt{4\pi(E+M)} \begin{pmatrix} \frac{ip}{E+M} j_{j+\frac{1}{2}}(pr) \Omega_{j,j+\frac{1}{2},m}(\theta, \phi) \\ j_{j-\frac{1}{2}}(pr) \Omega_{j,j-\frac{1}{2},m}(\theta, \phi) \end{pmatrix}, \quad (\text{A.41})$$

$$v_{-\varkappa,m}(\mathbf{r}, p) = \sqrt{4\pi(E+M)} \begin{pmatrix} \frac{p}{E+M} j_{j-\frac{1}{2}}(pr) \Omega_{j,j-\frac{1}{2},m}(\theta, \phi) \\ i j_{j+\frac{1}{2}}(pr) \Omega_{j,j+\frac{1}{2},m}(\theta, \phi) \end{pmatrix}, \quad (\text{A.42})$$

for the negative energy. Here, we use $\Omega_{j,\ell,m}$ instead of $\Omega_{\kappa,m}$ since we specify the sign of κ . Following the parity transformation of the spherical spinors, $P\Omega_{j,\ell,m} = (-1)^\ell \Omega_{j,\ell,m}$, the spherical-wave solutions change under the parity transformation as follows.

$$Pu_{\varkappa,m}(\mathbf{r}, p) = (-1)^{j+\frac{1}{2}} \beta u_{\varkappa,m}(\mathbf{r}, p), \quad Pv_{\varkappa,m}(\mathbf{r}, p) = (-1)^{j+\frac{1}{2}} \beta v_{\varkappa,m}(\mathbf{r}, p), \quad (\text{A.43})$$

$$Pu_{-\varkappa,m}(\mathbf{r}, p) = (-1)^{j-\frac{1}{2}} \beta u_{-\varkappa,m}(\mathbf{r}, p), \quad Pv_{-\varkappa,m}(\mathbf{r}, p) = (-1)^{j-\frac{1}{2}} \beta v_{-\varkappa,m}(\mathbf{r}, p). \quad (\text{A.44})$$

Here, β is one of the Dirac matrices.

Now, we consider the partial-wave expansion for the Dirac spinors. We choose the coordinate for the spherical harmonics so that the incoming momentum \mathbf{p} is aligned with the (positive) z -axis. We recall that, in this coordinate, the partial-wave expansion of the plane-wave solution for the Schrödinger equation is given by

$$e^{ipr \cos \theta} = \sum_{\ell=0}^{\infty} i^\ell (2\ell+1) j_\ell(pr) P_\ell(\cos \theta), \quad e^{-ipr \cos \theta} = \sum_{\ell=0}^{\infty} i^\ell (2\ell+1) j_\ell(pr) P_\ell(-\cos \theta). \quad (\text{A.45})$$

This expansion may be rewritten in terms of the spherical harmonics by using a relation:

$$P_\ell(\cos \theta) = \sqrt{\frac{4\pi}{2\ell+1}} Y_{\ell,0}(\theta, \phi). \quad (\text{A.46})$$

The partial-wave expansion of the plane-wave Dirac solutions must have the following form:

$$\begin{aligned} u(\mathbf{p}, \chi) e^{ipr \cos \theta} &= \sum_{\varkappa=1}^{\infty} [a_{\varkappa,m} u_{\varkappa,m}(\mathbf{r}, p) + b_{\varkappa,m} u_{-\varkappa,m}(\mathbf{r}, p)], \\ v(\mathbf{p}, \chi) e^{-ipr \cos \theta} &= \sum_{\varkappa=1}^{\infty} [\bar{a}_{\varkappa,m} v_{\varkappa,m}(\mathbf{r}, p) + \bar{b}_{\varkappa,m} v_{-\varkappa,m}(\mathbf{r}, p)], \end{aligned} \quad (\text{A.47})$$

where $a_{\varkappa,m}$, $\bar{a}_{\varkappa,m}$, $b_{\varkappa,m}$ and $\bar{b}_{\varkappa,m}$ are the expansion coefficients. Since the left-hand side depends only on $\cos \theta$, the right-hand side should contain only the terms proportional to $Y_{\ell,0}$. In other words, we choose the expansion coefficients to satisfy this condition.

We consider the positive-energy solution (A.33) with up-spin $m_s = 1/2$ as an example. For this case, the upper component of the two-component spinor should be proportional to $Y_{\ell,0}$, namely $m = 1/2$ in the right-hand side. Both upper and lower two-component spinors of a linear combination $u_{\varkappa,\frac{1}{2}}(\mathbf{r}, p) + u_{-\varkappa,\frac{1}{2}}(\mathbf{r}, p)$ (with a positive \varkappa) are proportional to a linear combination of spherical spinors:

$$-i j_{j+\frac{1}{2}}(pr) \Omega_{j,j+\frac{1}{2},\frac{1}{2}} + j_{j-\frac{1}{2}}(pr) \Omega_{j,j-\frac{1}{2},\frac{1}{2}}. \quad (\text{A.48})$$

Choosing $a_{\kappa,m} = b_{\kappa,m} = i^{\kappa-1}\sqrt{\kappa}$ and summing over κ , the upper component remains while the lower component vanishes. As a result, one finds the summation is proportional to $u(\mathbf{p}, \chi_{1/2})$. In a similar way, we obtain the partial-wave expansion of the other plane-wave solutions:

$$\begin{aligned}
u\left(\mathbf{p}, \chi_{\frac{1}{2}}\right) e^{ipr \cos \theta} &= \sum_{\kappa=1}^{\infty} i^{\kappa-1} \sqrt{\kappa} \left[u_{\kappa, \frac{1}{2}}(\mathbf{r}, p) + u_{-\kappa, \frac{1}{2}}(\mathbf{r}, p) \right] \\
u\left(\mathbf{p}, \chi_{-\frac{1}{2}}\right) e^{ipr \cos \theta} &= \sum_{\kappa=1}^{\infty} i^{\kappa-1} \sqrt{\kappa} \left[-u_{\kappa, -\frac{1}{2}}(\mathbf{r}, p) + u_{-\kappa, -\frac{1}{2}}(\mathbf{r}, p) \right], \\
v\left(\mathbf{p}, \chi_{\frac{1}{2}}\right) e^{-ipr \cos \theta} &= \sum_{\kappa=1}^{\infty} (-i)^{\kappa-1} \sqrt{\kappa} \left[v_{\kappa, \frac{1}{2}}(\mathbf{r}, p) + v_{-\kappa, \frac{1}{2}}(\mathbf{r}, p) \right], \\
v\left(\mathbf{p}, \chi_{-\frac{1}{2}}\right) e^{-ipr \cos \theta} &= \sum_{\kappa=1}^{\infty} (-i)^{\kappa-1} \sqrt{\kappa} \left[-v_{\kappa, -\frac{1}{2}}(\mathbf{r}, p) + v_{-\kappa, -\frac{1}{2}}(\mathbf{r}, p) \right].
\end{aligned} \tag{A.49}$$

One may consider other combinations that are orthogonal to the above combinations. One finds that the sum of these combinations gives the parity-transformed plane-wave solutions.

$$\begin{aligned}
\beta u\left(\mathbf{p}, \frac{1}{2}\right) e^{-ipr \cos \theta} &= \sum_{\kappa=1}^{\infty} (-i)^{\kappa-1} \sqrt{\kappa} \left[-u_{\kappa, \frac{1}{2}}(\mathbf{r}, p) + u_{-\kappa, \frac{1}{2}}(\mathbf{r}, p) \right], \\
\beta u\left(\mathbf{p}, -\frac{1}{2}\right) e^{-ipr \cos \theta} &= \sum_{\kappa=1}^{\infty} (-i)^{\kappa-1} \sqrt{\kappa} \left[u_{\kappa, -\frac{1}{2}}(\mathbf{r}, p) + u_{-\kappa, -\frac{1}{2}}(\mathbf{r}, p) \right], \\
-\beta v\left(\mathbf{p}, \frac{1}{2}\right) e^{ipr \cos \theta} &= \sum_{\kappa=1}^{\infty} i^{\kappa-1} \sqrt{\kappa} \left[-v_{\kappa, \frac{1}{2}}(\mathbf{r}, p) + v_{-\kappa, \frac{1}{2}}(\mathbf{r}, p) \right], \\
-\beta v\left(\mathbf{p}, -\frac{1}{2}\right) e^{ipr \cos \theta} &= \sum_{\kappa=1}^{\infty} i^{\kappa-1} \sqrt{\kappa} \left[v_{\kappa, -\frac{1}{2}}(\mathbf{r}, p) + v_{-\kappa, -\frac{1}{2}}(\mathbf{r}, p) \right].
\end{aligned} \tag{A.50}$$

B Matching Conditions of Wave-functions

In this appendix, we give calculations of the matching conditions for the wave functions discussed in Section 2 in detail.

B.1 Scattering on the infinitely large Q-ball wall

Now, we give the detail of the calculation of the matching conditions for the scattering of the colorless quarks on the infinitely large Q-ball wall in Section 2.1. First, we consider the case that the incoming quark is left-handed. The momentum assignments for the massless fermions and the massive fermions are given in Eqs. (2.16) and (2.17), and the scattering process is illustrated in Fig. 1. The projections operation which the constant spinors have to satisfy is shown in Eq. (2.19).

We solve the matching conditions for Weyl fermions with positive and negative frequency modes.

At the left boundary $z = -R$, the matching conditions for the positive frequency solutions give

$$\begin{aligned} & \sqrt{\sigma \cdot p} A_- e^{-ip \cdot x} + \sum_{s=\pm} \sqrt{\sigma \cdot p_{Bs}} B_s e^{-ip_{Bs} \cdot x} \\ &= \sum_{m=\pm} \left[\sin \beta \left(\sqrt{\sigma \cdot \kappa_D^m} e^{-i\kappa_D^m \cdot x} D^m \right) + \cos \beta \left(\sqrt{\sigma \cdot \kappa_F^m} e^{-i\kappa_F^m \cdot x} F^m \right) \right] e^{-i\omega t}, \end{aligned} \quad (\text{B.1})$$

$$\begin{aligned} & \sqrt{\sigma \cdot \kappa_B} G_B e^{-i\kappa_B \cdot x} \\ &= \sum_{m=\pm} \left[\cos \beta \left(\sqrt{\sigma \cdot \kappa_D^m} e^{-i\kappa_D^m \cdot x} D^m \right) - \sin \beta \left(\sqrt{\sigma \cdot \kappa_F^m} e^{-i\kappa_F^m \cdot x} F^m \right) \right]. \end{aligned} \quad (\text{B.2})$$

Here, A and B_\pm denote the spinors for the incoming and reflected quarks, G_B is the spinor for the gluino, and D^\pm and F^\pm denotes the spinors for the fermions inside the Q-ball. x denotes the four-vector of any position on the left boundary. We note that the wave function inside the Q-ball corresponding to the quark is multiplied by the time-dependent phase factor $e^{-i\omega t}$. We remind that the subscript of B_\pm indicates its spin direction while the superscripts of D^\pm and F^\pm indicate whether the decaying mode or the growing mode. On the other hand, the matching conditions for the negative frequency solutions gives

$$\begin{aligned} & \sqrt{\bar{\sigma} \cdot p} A_- e^{-ip \cdot x} + \sum_{s=\pm} \sqrt{\bar{\sigma} \cdot p_{Bs}} B_s e^{-ip_{Bs} \cdot x} \\ &= \sum_{m=\pm} \left[\sin \beta \left(\sqrt{\bar{\sigma} \cdot \kappa_D^m} e^{-i\kappa_D^m \cdot x} D^m \right) + \cos \beta \left(-\sqrt{\bar{\sigma} \cdot \kappa_F^m} e^{-i\kappa_F^m \cdot x} F^m \right) \right] e^{i\omega t}, \end{aligned} \quad (\text{B.3})$$

$$\begin{aligned} & \sqrt{\bar{\sigma} \cdot \kappa_B} G_B e^{-i\kappa_B \cdot x} \\ &= \sum_{m=\pm} \left[\cos \beta \left(\sqrt{\bar{\sigma} \cdot \kappa_D^m} e^{-i\kappa_D^m \cdot x} D^m \right) - \sin \beta \left(-\sqrt{\bar{\sigma} \cdot \kappa_F^m} e^{-i\kappa_F^m \cdot x} F^m \right) \right]. \end{aligned} \quad (\text{B.4})$$

Here, we take the complex conjugate of the negative frequency solutions using Eq. (A.3). The negative sign in front of F^m originates from the relative sign of the Majorana wave function for negative mass in Eq. (2.13). At the right boundary $z = R$, the matching conditions for the positive and negative frequency solutions give

$$\sum_s \sqrt{\sigma \cdot p_{Cs}} C_s e^{-ip_{Cs} \cdot x'} = \sum_m \left[\sin \beta \left(\sqrt{\sigma \cdot \kappa_D^m} e^{-i\kappa_D^m \cdot x'} D^m \right) + \cos \beta \left(\sqrt{\sigma \cdot \kappa_F^m} e^{-i\kappa_F^m \cdot x'} F^m \right) \right] e^{-i\omega t}, \quad (\text{B.5})$$

$$\sqrt{\sigma \cdot \kappa_C} G_C e^{-i\kappa_C \cdot x'} = \sum_m \left[\cos \beta \left(\sqrt{\sigma \cdot \kappa_D^m} e^{-i\kappa_D^m \cdot x'} D^m \right) - \sin \beta \left(\sqrt{\sigma \cdot \kappa_F^m} e^{-i\kappa_F^m \cdot x'} F^m \right) \right], \quad (\text{B.6})$$

$$\sum_s \sqrt{\bar{\sigma} \cdot p_{Cs}} C_s e^{-ip_{Cs} \cdot x'} = \sum_m \left[\sin \beta \left(\sqrt{\bar{\sigma} \cdot \kappa_D^m} e^{-i\kappa_D^m \cdot x'} D^m \right) + \cos \beta \left(-\sqrt{\bar{\sigma} \cdot \kappa_F^m} e^{-i\kappa_F^m \cdot x'} F^m \right) \right] e^{i\omega t}, \quad (\text{B.7})$$

$$\sqrt{\bar{\sigma} \cdot \kappa_C} G_C e^{-i\kappa_C \cdot x'} = \sum_m \left[\cos \beta \left(\sqrt{\bar{\sigma} \cdot \kappa_D^m} e^{-i\kappa_D^m \cdot x'} D^m \right) - \sin \beta \left(-\sqrt{\bar{\sigma} \cdot \kappa_F^m} e^{-i\kappa_F^m \cdot x'} F^m \right) \right]. \quad (\text{B.8})$$

Here, x' denotes the four-vector of any position on the right boundary.

We ignore the momentum along the Q-ball wall when the injected momentum is assumed to be sufficiently smaller than the masses of the fermions. Since all the massive fermions have the

same energy, $E - \omega$, the matching conditions for the gluino wave function at the right boundary are rewritten as the time-independent form as follows.

$$2\sqrt{M}G_B e^{-MR} = 2\sqrt{M_+} \cos \beta e^{-M_+R} D^+ - 2\sqrt{M_-} \sin \beta e^{-M_-R} F^+ \\ - 2i\sigma^3 \sqrt{M_+} \cos \beta e^{M_+R} D^- + 2i\sigma^3 \sqrt{M_-} \sin \beta e^{M_-R} F^- , \quad (\text{B.9})$$

$$2\sqrt{M}G_B e^{-MR} = 2\sqrt{M_+} \cos \beta e^{-M_+R} D^+ + 2\sqrt{M_-} \sin \beta e^{-M_-R} F^+ \\ + 2i\sigma^3 \sqrt{M_+} \cos \beta e^{M_+R} D^- + 2i\sigma^3 \sqrt{M_-} \sin \beta e^{M_-R} F^- . \quad (\text{B.10})$$

In a similar way, the matching conditions for the gluino wave function at left boundary are rewritten in the time-independent form as follows.

$$2\sqrt{M}G_C e^{-MR} = 2i\sigma^3 \sqrt{M_+} \cos \beta e^{M_+R} D^+ - 2i\sigma^3 \sqrt{M_-} \sin \beta e^{M_-R} F^+ \\ + 2\sqrt{M_+} \cos \beta e^{-M_+R} D^- - 2\sqrt{M_-} \sin \beta e^{-M_-R} F^- , \quad (\text{B.11})$$

$$2\sqrt{M}G_C e^{-MR} = -2i\sigma^3 \sqrt{M_+} \cos \beta e^{M_+R} D^+ - 2i\sigma^3 \sqrt{M_-} \sin \beta e^{M_-R} F^+ \\ + 2\sqrt{M_+} \cos \beta e^{-M_+R} D^- + 2\sqrt{M_-} \sin \beta e^{-M_-R} F^- . \quad (\text{B.12})$$

By removing the spinors of gluino, G_B and G_C , we find the relations between the spinors D^\pm and F^\mp as follows.

$$D^- = i\sigma^3 \sqrt{\frac{M_-}{M_+}} \tan \beta e^{-(M_++M_-)R} F^+ , \quad (\text{B.13})$$

$$D^+ = -i\sigma^3 \sqrt{\frac{M_-}{M_+}} \tan \beta e^{-(M_++M_-)R} F^- . \quad (\text{B.14})$$

We replace D^\pm in the matching conditions for quark wave functions with F^\pm . Considering the matching conditions for C_\pm , we give the constant spinors F^\pm in terms of C_\pm . All the time-dependent factor is $e^{-i(E-\omega)t}$ thanks to our momentum assignment and helicity, and hence the system of equations is closed.

$$2\sqrt{E} e^{-i\theta \frac{\sigma^2}{2}} \bar{C}_- e^{iE \cos \theta R} = \sqrt{M_-} \cos \beta (\mathbb{1} + i\sigma^3) (1 + e^{-2(M_++M_-)R} \tan^2 \beta) e^{M_-R} F^+ \\ + \sqrt{M_-} \cos \beta (\mathbb{1} - i\sigma^3) (1 + \tan^2 \beta) e^{-M_-R} F^- , \quad (\text{B.15})$$

$$2\sqrt{E - 2\omega} e^{-i\theta' \frac{\sigma^2}{2}} \bar{C}_+ e^{i(E-2\omega) \cos \theta' R} = -\sqrt{M_-} \cos \beta (\mathbb{1} - i\sigma^3) (1 + e^{-2(M_++M_-)R} \tan^2 \beta) e^{M_-R} F^+ \\ - \sqrt{M_-} \cos \beta (\mathbb{1} + i\sigma^3) (1 + \tan^2 \beta) e^{-M_-R} F^- . \quad (\text{B.16})$$

We define the spinors for the transmitted quarks projected onto the z -axis (spinors with bars) as follows.

$$\bar{C}_- \equiv e^{i\theta \frac{\sigma^2}{2}} C_- , \quad \bar{C}_+ \equiv e^{i\theta' \frac{\sigma^2}{2}} C_+ . \quad (\text{B.17})$$

Due to the projections, \bar{C}_\pm satisfy $(\mathbb{1} \pm \sigma^3) \bar{C}_\mp = 0$ and $(\mathbb{1} \pm \sigma^3) \bar{C}_\pm = 2\bar{C}_\pm$. We multiply $(\mathbb{1} \pm i\sigma^3)$

to make the F^\pm terms proportional to $\mathbb{1}$. F^\pm are given as a function of \bar{C}_\pm as follows.

$$\begin{aligned} & 2(1 + \tan^2 \beta) \sqrt{M_-} \cos \beta (-i\sigma^3) e^{-M_- R} F^- \\ &= \sqrt{E} (1 - i\sigma^3) e^{-i\theta \frac{\sigma^2}{2}} \bar{C}_- e^{iER} + \sqrt{E - 2\omega} (1 + i\sigma^3) e^{-i\theta' \frac{\sigma^2}{2}} \bar{C}_+ e^{i(E-2\omega)R}, \end{aligned} \quad (\text{B.18})$$

$$\begin{aligned} & 2(1 + e^{-2(M_++M_-)R} \tan^2 \beta) \sqrt{M_-} \cos \beta e^{M_- R} F^+ \\ &= \sqrt{E} (1 - i\sigma^3) e^{-i\theta \frac{\sigma^2}{2}} \bar{C}_- e^{iER} - \sqrt{E - 2\omega} (1 + i\sigma^3) e^{-i\theta' \frac{\sigma^2}{2}} \bar{C}_+ e^{i(E-2\omega)R}. \end{aligned} \quad (\text{B.19})$$

Similarly to \bar{C}_\pm , we define the spinors for the massless quarks projected onto the z -axis (spinors with bars) as follows.

$$\bar{A}_- \equiv e^{i\theta \frac{\sigma^2}{2}} A_-, \quad \bar{B}_- \equiv e^{-i\theta' \frac{\sigma^2}{2}} B_-, \quad \bar{B}_+ \equiv e^{-i\theta \frac{\sigma^2}{2}} B_+. \quad (\text{B.20})$$

We note that $(\mathbb{1} + \sigma^3) \bar{A}_- = 0$ and $(\mathbb{1} \mp \sigma^3) \bar{B}_\pm = 0$, and $(\mathbb{1} - \sigma^3) \bar{A}_- = 2\bar{A}_-$ and $(\mathbb{1} \pm \sigma^3) \bar{B}_\pm = 2\bar{B}_\pm$. The matching conditions for the massless quarks at $z = -R$ are simplified as follows.

$$\begin{aligned} & 2\sqrt{E} e^{-i\theta \frac{\sigma^2}{2}} \bar{A}_- e^{-iE \cos \theta R} + 2\sqrt{E} e^{i\theta \frac{\sigma^2}{2}} \bar{B}_+ e^{iE \cos \theta R} \\ &= \sqrt{M_-} \cos \beta (\mathbb{1} + i\sigma^3) (1 + \tan^2 \beta) e^{-M_- R} F^+ \\ &\quad + \sqrt{M_-} \cos \beta (\mathbb{1} - i\sigma^3) (1 + e^{-2(M_++M_-)R} \tan^2 \beta) e^{M_- R} F^-, \end{aligned} \quad (\text{B.21})$$

$$\begin{aligned} & 2\sqrt{E - 2\omega} e^{i\theta' \frac{\sigma^2}{2}} \bar{B}_- e^{i(E-2\omega) \cos \theta' R} \\ &= -\sqrt{M_-} \cos \beta (\mathbb{1} - i\sigma^3) (1 + \tan^2 \beta) e^{-M_- R} F^+ \\ &\quad - \sqrt{M_-} \cos \beta (\mathbb{1} + i\sigma^3) (1 + e^{-2(M_++M_-)R} \tan^2 \beta) e^{M_- R} F^-. \end{aligned} \quad (\text{B.22})$$

The spinor F^\pm is given in terms of a function of \bar{C}_\pm . We obtain the spinor relations among quarks by inserting F^\pm as follows:

$$\begin{aligned} & \sqrt{E} e^{-i\theta \frac{\sigma^2}{2}} \bar{A}_- e^{-iER \cos \theta} + \sqrt{E} e^{i\theta \frac{\sigma^2}{2}} \bar{B}_+ e^{iER \cos \theta} \\ &= \frac{a_-}{4} \sqrt{E - 2\omega} (i\sigma^3) e^{-i\theta' \frac{\sigma^2}{2}} \bar{C}_+ e^{i(E-2\omega)R \cos \theta'} + \frac{a_+}{4} = \sqrt{E} e^{-i\theta \frac{\sigma^2}{2}} \bar{C}_- e^{iER \cos \theta}, \end{aligned} \quad (\text{B.23})$$

$$\begin{aligned} & \sqrt{E - 2\omega} (i\sigma^3) e^{i\theta' \frac{\sigma^2}{2}} \bar{B}_- e^{i(E-2\omega)R} \\ &= \frac{a_+}{4} \sqrt{E - 2\omega} (i\sigma^3) e^{-i\theta' \frac{\sigma^2}{2}} \bar{C}_+ e^{i(E-2\omega)R \cos \theta'} + \frac{a_-}{4} \sqrt{E} e^{-i\theta \frac{\sigma^2}{2}} \bar{C}_- e^{iER \cos \theta}. \end{aligned} \quad (\text{B.24})$$

Here, we define the parameters a_\pm as follows.

$$a_\pm = \frac{1 + e^{-2(M_++M_-)R} \tan^2 \beta}{1 + \tan^2 \beta} e^{2M_- R} \pm \frac{1 + \tan^2 \beta}{1 + e^{-2(M_++M_-)R} \tan^2 \beta} e^{-2M_- R}. \quad (\text{B.25})$$

We take the large R limit in the following and keep the dominant terms in order to simplify the solutions. The matching conditions for quarks at the right-side boundary of the Q-ball are simplified as follows.

$$\begin{aligned} & 2\sqrt{M_-} \cos \beta (1 + \tan^2 \beta) (-i\sigma^3) e^{-M_- R} F^- \\ &= \sqrt{E} (1 - i\sigma^3) e^{-i\theta \frac{\sigma^2}{2}} \bar{C}_- e^{iER \cos \theta} + \sqrt{E - 2\omega} (1 + i\sigma^3) e^{-i\theta' \frac{\sigma^2}{2}} \bar{C}_+ e^{i(E-2\omega)R \cos \theta'}, \end{aligned} \quad (\text{B.26})$$

$$\begin{aligned} & 2\sqrt{M_-} \cos \beta e^{M_- R} F^+ \\ &= \sqrt{E} (1 - i\sigma^3) e^{-i\theta \frac{\sigma^2}{2}} \bar{C}_- e^{iER \cos \theta} - \sqrt{E - 2\omega} (1 + i\sigma^3) e^{-i\theta' \frac{\sigma^2}{2}} \bar{C}_+ e^{i(E-2\omega)R \cos \theta'}. \end{aligned} \quad (\text{B.27})$$

Meanwhile, the matching conditions for quarks at the left-side boundary of the Q-ball are simplified as follows.

$$\begin{aligned} & \sqrt{E}(\mathbb{1} - i\sigma^3)e^{-i\theta\frac{\sigma^2}{2}}\bar{A}_-e^{-iER\cos\theta} + \sqrt{E}(\mathbb{1} - i\sigma^3)e^{i\theta\frac{\sigma^2}{2}}\bar{B}_+e^{iER\cos\theta} \\ &= \sqrt{M_-}\cos\beta(1 + \tan^2\beta)e^{-M_-R}F^+ + \sqrt{M_-}\cos\beta(-i\sigma^3)e^{M_-R}F^-, \end{aligned} \quad (\text{B.28})$$

$$\begin{aligned} & \sqrt{E-2\omega}(\mathbb{1} + i\sigma^3)e^{i\theta'\frac{\sigma^2}{2}}\bar{B}_-e^{i(E-2\omega)R\cos\theta'} \\ &= -\sqrt{M_-}\cos\beta(1 + \tan^2\beta)e^{-M_-R}F^+ - \sqrt{M_-}\cos\beta(i\sigma^3)e^{M_-R}F^-. \end{aligned} \quad (\text{B.29})$$

Then, we obtain the spinor relations among the massless quarks by removing the spinor F^\pm as follows. We also simplify the relations by multiplying $1 \pm i\sigma^3$.

$$\begin{aligned} & \sqrt{E}e^{-i\theta\frac{\sigma^2}{2}}\bar{A}_-e^{-iER\cos\theta} + \sqrt{E}e^{i\theta\frac{\sigma^2}{2}}\bar{B}_+e^{iER\cos\theta} \\ &= \frac{e^{2M_-R}}{2(1 + \tan^2\beta)} \left[\sqrt{E}e^{-i\theta\frac{\sigma^2}{2}}\bar{C}_-e^{iER\cos\theta} + \sqrt{E-2\omega}(i\sigma^3)e^{-i\theta'\frac{\sigma^2}{2}}\bar{C}_+e^{i(E-2\omega)R\cos\theta'} \right], \end{aligned} \quad (\text{B.30})$$

$$\begin{aligned} & \sqrt{E-2\omega}e^{i\theta'\frac{\sigma^2}{2}}\bar{B}_-e^{i(E-2\omega)R\cos\theta'} \\ &= \frac{e^{2M_-R}}{2(1 + \tan^2\beta)} \left[\sqrt{E}(-i\sigma^3)e^{-i\theta\frac{\sigma^2}{2}}\bar{C}_-e^{iER\cos\theta} + \sqrt{E-2\omega}e^{-i\theta'\frac{\sigma^2}{2}}\bar{C}_+e^{i(E-2\omega)R\cos\theta'} \right]. \end{aligned} \quad (\text{B.31})$$

Since the spinors with bars are the eigenstate of σ^3 , each spinor has only single component, either upper or lower component: only lower component for \bar{B}_- and \bar{C}_- , while only upper component for \bar{C}_+ . We multiply $e^{-i\theta'\frac{\sigma^2}{2}}$ both relations and expand the rotation factors $e^{-i(\theta-\theta')\frac{\sigma^2}{2}}$ and $e^{-i\theta'\sigma^2}$ in σ^2 . We obtain two spinor relations from the relation for \bar{B}_- by comparing the upper and lower components as follow.

$$\begin{aligned} \sqrt{E-2\omega}\bar{B}_-e^{i(E-2\omega)R\cos\theta'} &= \frac{e^{2M_-R}}{2(1 + \tan^2\beta)}\sqrt{E}(-i\sigma^3)\cos\frac{\theta-\theta'}{2}\bar{C}_-e^{iER\cos\theta} \\ &+ \frac{e^{2M_-R}}{2(1 + \tan^2\beta)}\sqrt{E-2\omega}(-i\sin\theta')\sigma^2\bar{C}_+e^{i(E-2\omega)R\cos\theta'}, \end{aligned} \quad (\text{B.32})$$

$$\begin{aligned} 0 &= \frac{e^{2M_-R}}{2(1 + \tan^2\beta)}\sqrt{E}(-i\sigma^3)\left(-i\sin\frac{\theta-\theta'}{2}\right)\sigma^2\bar{C}_-e^{iER\cos\theta} \\ &+ \frac{e^{2M_-R}}{2(1 + \tan^2\beta)}\sqrt{E-2\omega}\cos\theta'\bar{C}_+e^{i(E-2\omega)R\cos\theta'}. \end{aligned} \quad (\text{B.33})$$

We also obtain two spinor relations from the first equation by the similar procedure.

$$\begin{aligned} & \sqrt{E}\bar{A}_-e^{-iER\cos\theta} + \sqrt{E}(i\sin\theta)\sigma^2\bar{B}_+e^{iER\cos\theta} \\ &= \frac{e^{2M_-R}}{2(1 + \tan^2\beta)} \left[\sqrt{E}\bar{C}_-e^{iER\cos\theta} + \sqrt{E-2\omega}\left(-i\sin\frac{\theta+\theta'}{2}\right)(i\sigma^3\sigma^2)\bar{C}_+e^{i(E-2\omega)R\cos\theta'} \right], \end{aligned} \quad (\text{B.34})$$

$$\sqrt{E}\cos\theta\bar{B}_+e^{iER\cos\theta} = \frac{e^{2M_-R}}{2(1 + \tan^2\beta)} \left[\sqrt{E-2\omega}\left(\cos\frac{\theta+\theta'}{2}\right)(i\sigma^3)\bar{C}_+e^{i(E-2\omega)R\cos\theta'} \right], \quad (\text{B.35})$$

These four equations give the spinors \bar{B}_\pm and \bar{C}_\pm in terms of the spinor \bar{A}_- .

$$\sqrt{E}\bar{B}_+e^{iER\cos\theta} = \frac{\sin\left(\frac{\theta-\theta'}{2}\right)}{\cos\left(\frac{\theta+\theta'}{2}\right)}(i\sigma^2)\sqrt{E}\bar{A}_-e^{-iER\cos\theta}, \quad (\text{B.36})$$

$$\sqrt{E-2\omega}\bar{B}_-e^{i(E-2\omega)R\cos\theta} = i\frac{\cos\theta}{\cos\left(\frac{\theta+\theta'}{2}\right)}\sqrt{E}\bar{A}_-e^{-iER\cos\theta}, \quad (\text{B.37})$$

$$\sqrt{E-2\omega}\bar{C}_+e^{i(E-2\omega)R\cos\theta} = 2e^{-M-R}(1+\tan^2\beta)\frac{\cos\theta\sin\left(\frac{\theta-\theta'}{2}\right)}{\cos^2\left(\frac{\theta+\theta'}{2}\right)}\sigma^2\sqrt{E}\bar{A}_-e^{-iER\cos\theta}, \quad (\text{B.38})$$

$$\sqrt{E}\bar{C}_-e^{iER\cos\theta} = 2e^{-M-R}(1+\tan^2\beta)\frac{\cos\theta\cos\theta'}{\cos^2\left(\frac{\theta+\theta'}{2}\right)}\sqrt{E}\bar{A}_-e^{-iER\cos\theta}, \quad (\text{B.39})$$

As discussed in the text, we can consider the scattering with normal incident by taking $\theta = \theta' = 0$ and find $B_+ = C_+ = 0$ and Eqs. (2.27) and (2.28).

We also obtain the spinors for the massive fermions in terms of the incoming spinor A_- . We show the spinors in the large R limit as confirmation that the matching conditions are solved in a self-consistent way. As for the Majorana fermions inside the Q-ball, we get

$$\sqrt{M_+}\sin\beta D^+ = (1+i)\frac{\cos\theta}{\cos\left(\frac{\theta+\theta'}{2}\right)}\tan^2\beta e^{-(2M_-+M_+)R}\left(\cos\frac{\theta'}{2}-\sin\frac{\theta'}{2}\sigma^2\right)\sqrt{E}\bar{A}_-e^{-iER\cos\theta}, \quad (\text{B.40})$$

$$\sqrt{M_+}\sin\beta D^- = -(1-i)\frac{\cos\theta}{\cos^2\left(\frac{\theta+\theta'}{2}\right)}\tan^2\beta(1+\tan^2\beta)e^{-(4M_-+M_+)R}U\sqrt{E}\bar{A}_-e^{-iER\cos\theta}, \quad (\text{B.41})$$

$$\sqrt{M_-}\sin\beta F^+ = -(1+i)\frac{\cos\theta}{\cos^2\left(\frac{\theta+\theta'}{2}\right)}(1+\tan^2\beta)e^{-3M_-R}U\sqrt{E}\bar{A}_-e^{-iER\cos\theta}, \quad (\text{B.42})$$

$$\sqrt{M_-}\sin\beta F^- = (1-i)\frac{\cos\theta}{\cos\left(\frac{\theta+\theta'}{2}\right)}e^{-M-R}\left(\cos\frac{\theta'}{2}+\sin\frac{\theta'}{2}\sigma^2\right)\sqrt{E}\bar{A}_-e^{-iER\cos\theta}. \quad (\text{B.43})$$

Here, we define the rotation matrix U as follows.

$$U = \frac{1}{2}\left(\cos\frac{\theta}{2}-2\cos\frac{\theta-2\theta'}{2}-\cos\frac{\theta+2\theta'}{2}\right)-\frac{1}{2}\left(\sin\frac{\theta}{2}+2\sin\frac{\theta-2\theta'}{2}+\sin\frac{\theta+2\theta'}{2}\right)\sigma^2. \quad (\text{B.44})$$

As for the reflected gluino G_B and the transmitted gluino G_C , we get

$$\sqrt{M}G_B = -(1+i)\frac{\cos\theta}{\cos\left(\frac{\theta+\theta'}{2}\right)}\tan\beta\left(\cos\frac{\theta'}{2}-\sin\frac{\theta'}{2}\sigma^2\right)\sqrt{E}\bar{A}_-e^{-iER\cos\theta}, \quad (\text{B.45})$$

$$\sqrt{M}G_C = (1-i)\frac{\cos\theta}{\cos^2\left(\frac{\theta+\theta'}{2}\right)}\tan\beta(1+\tan^2\beta)e^{-2M-R}U\sqrt{E}\bar{A}_-e^{-iER\cos\theta}. \quad (\text{B.46})$$

Next, we consider the opposite helicity for the incoming quark, namely right-handed quark, and assign the four-momenta for each fermions as follows.

$$\begin{aligned} p &= (E, E\sin\theta, 0, E\cos\theta), \\ p_{B+} &= (E+2\omega, (E+2\omega)\sin\theta', 0, -(E+2\omega)\cos\theta'), & p_{B-} &= (E, E\sin\theta, 0, -E\cos\theta), \\ p_{C+} &= (E, E\sin\theta, 0, E\cos\theta), & p_{C-} &= (E+2\omega, (E+2\omega)\sin\theta', 0, (E+2\omega)\cos\theta'), \\ \kappa_B &= (E+\omega, E\sin\theta, 0, -iM), & \kappa_C &= (E+\omega, E\sin\theta, 0, iM), \\ \kappa_D^\pm &= (E+\omega, E\sin\theta, 0, \mp iM_\pm), & \kappa_F^\pm &= (E+\omega, E\sin\theta, 0, \mp iM_-). \end{aligned} \quad (\text{B.47})$$

The helicity projections operations that the massless spinors (with the projection onto z -axis) are

$$\begin{aligned}\frac{1}{2}(\mathbb{1} - \sigma^3)e^{i\theta\frac{\sigma^2}{2}}A_+ &= 0, \\ \frac{1}{2}(\mathbb{1} + \sigma^3)e^{-i\theta\frac{\sigma^2}{2}}B_- &= 0, & \frac{1}{2}(\mathbb{1} - \sigma^3)e^{-i\theta'\frac{\sigma^2}{2}}B_+ &= 0, \\ \frac{1}{2}(\mathbb{1} + \sigma^3)e^{i\theta'\frac{\sigma^2}{2}}C_- &= 0, & \frac{1}{2}(\mathbb{1} - \sigma^3)e^{i\theta\frac{\sigma^2}{2}}C_+ &= 0,\end{aligned}\tag{B.48}$$

and the relation between the angles θ and θ' is given by

$$\frac{\sin \theta'}{\sin \theta} = \frac{E}{E + 2\omega}.\tag{B.49}$$

When the injected momentum is sufficiently smaller than the masses of the fermions, we have the same matching conditions as before. Therefore, we have the same relations between D^\pm and F^\mp as given in Eqs. (B.13) and (B.14)

We define the spinors for the transmitted quarks projected onto the z -axis (spinors with bars) as follows.

$$\bar{C}_- \equiv e^{i\theta'\frac{\sigma^2}{2}}C_-, \quad \bar{C}_+ \equiv e^{i\theta\frac{\sigma^2}{2}}C_+.\tag{B.50}$$

We note that the spinors with bars are different from those in the previous case since the energy for each helicity is also different from those in the previous case. Due to the projections, \bar{C}_\pm satisfy $(\mathbb{1} \pm \sigma^3)\bar{C}_\mp = 0$ and $(\mathbb{1} \pm \sigma^3)\bar{C}_\pm = 2\bar{C}_\pm$. Therefore, the matching condition for quarks at the right-side boundary of the Q-ball is written as follows.

$$\begin{aligned}2\sqrt{E+2\omega}e^{-i\theta'\frac{\sigma^2}{2}}\bar{C}_-e^{i(E+2\omega)\cos\theta'R} &= \sqrt{M_-}\cos\beta(\mathbb{1} + i\sigma^3)(1 + e^{-2(M_++M_-)R}\tan^2\beta)e^{M_-R}F^+ \\ &\quad + \sqrt{M_-}\cos\beta(\mathbb{1} - i\sigma^3)(1 + \tan^2\beta)e^{-M_-R}F^-, \end{aligned}\tag{B.51}$$

$$\begin{aligned}2\sqrt{E}e^{-i\theta\frac{\sigma^2}{2}}\bar{C}_+e^{iE\cos\theta R} &= -\sqrt{M_-}\cos\beta(\mathbb{1} - i\sigma^3)(1 + e^{-2(M_++M_-)R}\tan^2\beta)e^{M_-R}F^+ \\ &\quad - \sqrt{M_-}\cos\beta(\mathbb{1} + i\sigma^3)(1 + \tan^2\beta)e^{-M_-R}F^-. \end{aligned}\tag{B.52}$$

Similarly to the previous case, by multiplying $(\mathbb{1} \pm i\sigma^3)$ to make the F^+ terms proportional to $\mathbb{1}$, F^\pm are given as a function of \bar{C}_\pm as follows.

$$\begin{aligned}2(1 + \tan^2\beta)\sqrt{M_-}\cos\beta(-i\sigma^3)e^{-M_-R}F^- \\ = \sqrt{E}(1 - i\sigma^3)e^{-i\theta'\frac{\sigma^2}{2}}\bar{C}_-e^{i(E+2\omega)R\cos\theta'} + \sqrt{E-2\omega}(1 + i\sigma^3)e^{-i\theta\frac{\sigma^2}{2}}\bar{C}_+e^{iER\cos\theta}, \end{aligned}\tag{B.53}$$

$$\begin{aligned}2(1 + e^{-2(M_++M_-)R}\tan^2\beta)\sqrt{M_-}\cos\beta e^{M_-R}F^+ \\ = \sqrt{E}(1 - i\sigma^3)e^{-i\theta'\frac{\sigma^2}{2}}\bar{C}_-e^{i(E+2\omega)R\cos\theta} - \sqrt{E-2\omega}(1 + i\sigma^3)e^{-i\theta\frac{\sigma^2}{2}}\bar{C}_+e^{iER\cos\theta}. \end{aligned}\tag{B.54}$$

Similarly to \bar{C}_\pm , we define the spinors for the massless quarks at the left-side of the Q-ball projected onto the z -axis (spinors with bars) as follows.

$$\bar{A}_+ \equiv e^{i\theta\frac{\sigma^2}{2}}A_+, \quad \bar{B}_- \equiv e^{-i\theta\frac{\sigma^2}{2}}B_-, \quad \bar{B}_+ \equiv e^{-i\theta'\frac{\sigma^2}{2}}B_+.\tag{B.55}$$

We note that the bar spinors satisfy $(\mathbb{1} - \sigma^3)\bar{A}_+ = 0$, $(\mathbb{1} + \sigma^3)\bar{A}_+ = \bar{A}_+$ and $(\mathbb{1} \mp \sigma^3)\bar{B}_\pm = 0$, $(\mathbb{1} \pm \sigma^3)\bar{B}_\pm = 2\bar{B}_\pm$. The matching conditions for the massless quarks at $z = -R$ are simplified as follows.

$$\begin{aligned} & 2\sqrt{E + 2\omega}e^{i\theta'\frac{\sigma^2}{2}}\bar{B}_+e^{i(E+2\omega)\cos\theta'R} \\ &= \sqrt{M_-}\cos\beta(\mathbb{1} + i\sigma^3)(1 + \tan^2\beta)e^{-M_-R}F^+ \\ & \quad + \sqrt{M_-}\cos\beta(\mathbb{1} - i\sigma^3)(1 + e^{-2(M_++M_-)R}\tan^2\beta)e^{M_-R}F^-, \end{aligned} \quad (\text{B.56})$$

$$\begin{aligned} & 2\sqrt{E}e^{-i\theta\frac{\sigma^2}{2}}\bar{A}_+e^{-iE\cos\theta R} + 2\sqrt{E}e^{i\theta\frac{\sigma^2}{2}}\bar{B}_-e^{iE\cos\theta R} \\ &= -\sqrt{M_-}\cos\beta(\mathbb{1} - i\sigma^3)(1 + \tan^2\beta)e^{-M_-R}F^+ \\ & \quad - \sqrt{M_-}\cos\beta(\mathbb{1} + i\sigma^3)(1 + e^{-2(M_++M_-)R}\tan^2\beta)e^{M_-R}F^-. \end{aligned} \quad (\text{B.57})$$

The spinor F^\pm is given in terms of a function of \bar{C}_\pm . We obtain the spinor relations among quarks by inserting F^\pm as follows:

$$\begin{aligned} & \sqrt{E + 2\omega}e^{i\theta'\frac{\sigma^2}{2}}\bar{B}_+e^{i(E-2\omega)R\cos\theta'} \\ &= \frac{a_+}{4}\sqrt{E + 2\omega}e^{-i\theta'\frac{\sigma^2}{2}}\bar{C}_-e^{i(E+2\omega)R\cos\theta'} + \frac{a_-}{4}\sqrt{E}(i\sigma^3)e^{-i\theta\frac{\sigma^2}{2}}\bar{C}_+e^{iER\cos\theta}, \end{aligned} \quad (\text{B.58})$$

$$\begin{aligned} & \sqrt{E}e^{-i\theta\frac{\sigma^2}{2}}\bar{A}_+e^{-iER\cos\theta} + \sqrt{E}e^{i\theta\frac{\sigma^2}{2}}\bar{B}_-e^{iER\cos\theta} \\ &= \frac{a_-}{4}\sqrt{E + 2\omega}(-i\sigma^3)e^{-i\theta'\frac{\sigma^2}{2}}\bar{C}_-e^{i(E+2\omega)R\cos\theta'} + \frac{a_+}{4}\sqrt{E}e^{-i\theta\frac{\sigma^2}{2}}\bar{C}_+e^{iER\cos\theta}. \end{aligned} \quad (\text{B.59})$$

As with the previous discussion, we take the large R limit and get the spinors for the massless quarks in terms of A_+ . The spinors F^\pm are given by

$$\begin{aligned} & 2\sqrt{M_-}\cos\beta(1 + \tan^2\beta)(-i\sigma^3)e^{-M_-R}F^- \\ &= \sqrt{E}(1 - i\sigma^3)e^{-i\theta'\frac{\sigma^2}{2}}\bar{C}_-e^{i(E+2\omega)R\cos\theta} + \sqrt{E - 2\omega}(1 + i\sigma^3)e^{-i\theta'\frac{\sigma^2}{2}}\bar{C}_+e^{iER\cos\theta}, \end{aligned} \quad (\text{B.60})$$

$$\begin{aligned} & 2\sqrt{M_-}\cos\beta e^{M_-R}F^+ \\ &= \sqrt{E + 2\omega}(1 - i\sigma^3)e^{-i\theta\frac{\sigma^2}{2}}\bar{C}_-e^{i(E+2\omega)R} - \sqrt{E}(1 + i\sigma^3)e^{-i\theta'\frac{\sigma^2}{2}}\bar{C}_+e^{iER\cos\theta}. \end{aligned} \quad (\text{B.61})$$

The matching conditions for quarks at the left-side boundary of the Q-ball are simplified as follows.

$$\begin{aligned} & \sqrt{E + 2\omega}(\mathbb{1} - i\sigma^3)e^{i\theta'\frac{\sigma^2}{2}}\bar{B}_+e^{i(E+2\omega)R\cos\theta'} \\ &= \sqrt{M_-}\cos\beta(1 + \tan^2\beta)e^{-M_-R}F^+ + \sqrt{M_-}\cos\beta(-i\sigma^3)e^{M_-R}F^-, \end{aligned} \quad (\text{B.62})$$

$$\begin{aligned} & \sqrt{E}(\mathbb{1} + i\sigma^3)e^{-i\theta\frac{\sigma^2}{2}}\bar{A}_-e^{-iER\cos\theta} + \sqrt{E}(\mathbb{1} + i\sigma^3)e^{i\theta\frac{\sigma^2}{2}}\bar{B}_-e^{iER\cos\theta} \\ &= -\sqrt{M_-}\cos\beta(1 + \tan^2\beta)e^{-M_-R}F^+ - \sqrt{M_-}\cos\beta(i\sigma^3)e^{M_-R}F^-. \end{aligned} \quad (\text{B.63})$$

The spinor relations among quarks are simplified as follows.

$$\begin{aligned} & \sqrt{E+2\omega}e^{i\theta'\frac{\sigma^2}{2}}\bar{B}_+e^{i(E+2\omega)R\cos\theta'} \\ &= \frac{e^{2M-R}}{2(1+\tan^2\beta)} \left[\sqrt{E+2\omega}e^{-i\theta'\frac{\sigma^2}{2}}\bar{C}_-e^{i(E+2\omega)R\cos\theta'} + \sqrt{E}(i\sigma^3)e^{-i\theta\frac{\sigma^2}{2}}\bar{C}_+e^{iER\cos\theta} \right], \end{aligned} \quad (\text{B.64})$$

$$\begin{aligned} & \sqrt{E}e^{-i\theta\frac{\sigma^2}{2}}\bar{A}_-e^{-iER\cos\theta} + \sqrt{E}e^{i\theta\frac{\sigma^2}{2}}\bar{B}_-e^{iER\cos\theta} \\ &= \frac{e^{2M-R}}{2(1+\tan^2\beta)} \left[\sqrt{E+2\omega}(-i\sigma^3)e^{-i\theta'\frac{\sigma^2}{2}}\bar{C}_-e^{i(E+2\omega)R\cos\theta'} + \sqrt{E}e^{-i\theta\frac{\sigma^2}{2}}\bar{C}_+e^{iER\cos\theta} \right]. \end{aligned} \quad (\text{B.65})$$

We find the solutions for the massless quarks as follows.

$$\sqrt{E+2\omega}\bar{B}_+e^{i(E+2\omega)R\cos\theta'} = i\frac{\cos\theta}{\cos\left(\frac{\theta+\theta'}{2}\right)}\sqrt{E}\bar{A}_+e^{-iER\cos\theta}, \quad (\text{B.66})$$

$$\sqrt{E}\bar{B}_-e^{iER\cos\theta} = \frac{\sin\left(\frac{\theta-\theta'}{2}\right)}{\cos\left(\frac{\theta+\theta'}{2}\right)}\sqrt{E}(-i\sigma^2)\bar{A}_+e^{-iER\cos\theta}, \quad (\text{B.67})$$

$$\sqrt{E}\bar{C}_+e^{iER\cos\theta} = 2e^{-M-R}(1+\tan^2\beta)\frac{\cos\theta\cos\theta'}{\cos^2\left(\frac{\theta+\theta'}{2}\right)}\sqrt{E}\bar{A}_+e^{-iER\cos\theta}, \quad (\text{B.68})$$

$$\sqrt{E+2\omega}\bar{C}_-e^{i(E+2\omega)R\cos\theta'} = 2e^{-M-R}(1+\tan^2\beta)\frac{\cos\theta\sin\left(\frac{\theta-\theta'}{2}\right)}{\cos^2\left(\frac{\theta+\theta'}{2}\right)}\sigma^2\sqrt{E}\bar{A}_+e^{-iER\cos\theta}, \quad (\text{B.69})$$

B.2 Spherical Wave Scattering

Now, we give the detail of the calculation of the matching conditions for the scattering of the colorless quarks with the finite-size Q-ball in Section 2.2. Since we use the spherical wave state, it is convenient to use the four-component fermions. In contrast to the previous appendix, a matching condition for the Dirac spinors give two equations corresponding to the upper and the lower components of the four-component fermions. Hence, once we have the solution for the Dirac spinor, it is trivial that the charge-conjugated solutions (required for Majorana fermions) satisfy the matching conditions.

The massless solution is given by a linear combination of the spherical Bessel functions. Therefore, the outgoing and incoming Dirac fermions are described by the spherical Hankel functions $h_\kappa^{(1)}(x)$ and $h_\kappa^{(2)}(x)$, which behave as e^{ix}/x and e^{-ix}/x at large x , respectively. We choose the overall coefficients of P_κ and Q_κ to be convenient for constructing the plain-wave solution in terms of the spinor spherical harmonics. The wave functions for the incoming quark A_κ and the reflected quark B_κ are given by

$$\begin{aligned} P_\varkappa^A(r) &= -\sqrt{E+M_A}rh_\varkappa^{(2)}(p_Ar)A_\varkappa, & Q_\varkappa^A(r) &= \frac{p_A}{\sqrt{E+M_A}}rh_{\varkappa-1}^{(2)}(p_Ar)A_\varkappa, \\ P_\varkappa^B(r) &= -\sqrt{E+M_B}rh_\varkappa^{(1)}(p_Br)B_\varkappa, & Q_\varkappa^B(r) &= \frac{p_B}{\sqrt{E+M_B}}rh_{\varkappa-1}^{(1)}(p_Br)B_\varkappa, \end{aligned} \quad (\text{B.70})$$

for positive integer \varkappa , and

$$\begin{aligned} P_{-\varkappa}^A(r) &= -i\sqrt{E+M_A}rh_{-\varkappa}^{(2)}(p_Ar)A_{-\varkappa}, & Q_{-\varkappa}^A(r) &= -i\frac{p_A}{\sqrt{E+M_A}}rh_{-\varkappa}^{(2)}(p_Ar)A_{-\varkappa}, \\ P_{-\varkappa}^B(r) &= -i\sqrt{E+M_B}rh_{-\varkappa}^{(1)}(p_Br)B_{-\varkappa}, & Q_{-\varkappa}^B(r) &= -i\frac{p_B}{\sqrt{E+M_B}}rh_{-\varkappa}^{(1)}(p_Br)B_{-\varkappa}, \end{aligned} \quad (\text{B.71})$$

for negative integer $-\kappa$. Here, $p_{A,B}^2 = E^2 - M_{A,B}^2 > 0$, and A_κ and B_κ denote the coefficients for the wave functions. Since we assume that the injected energy E is less than the gluino mass and the field value of the scalar field, the wave function for the heavy fermions is given by a linear combination of the modified spherical Bessel functions. Gluinos mediate outside the Q-ball and are written by the use of spherical Bessel functions if the energy of incoming quark is sufficiently large. The wave function of gluinos should be analytic at $r \rightarrow \infty$ and be described by the second kind of the modified Bessel function $k_n(x)$:

$$\begin{aligned} P_\kappa^C(r) &= -\sqrt{E + M_C} r k_\kappa(|p_C| r) C_\kappa, & Q_\kappa^C(r) &= -\frac{|p_C|}{\sqrt{E + M_C}} r k_{\kappa-1}(|p_C| r) C_\kappa, \\ P_{-\kappa}^C(r) &= -i\sqrt{E + M_C} r k_{-\kappa-1}(|p_C| r) C_{-\kappa}, & Q_{-\kappa}^C(r) &= -i\frac{|p_C|}{\sqrt{E + M_C}} r k_{-\kappa}(|p_C| r) C_{-\kappa}. \end{aligned} \quad (\text{B.72})$$

Here, $p_C^2 = E^2 - M_C^2 < 0$. The wave functions for the fermions in mass basis inside the Q-ball should be analytic at $r \rightarrow 0$, and hence the wave functions are described by the first kind of the modified Bessel function $i_n(x)$:

$$\begin{aligned} P_\kappa^D(r) &= -\sqrt{E + M_D} r i_\kappa(|p_D| r) D_\kappa, & Q_\kappa^D(r) &= -\frac{|p_D|}{\sqrt{E + M_D}} r i_{\kappa-1}(|p_D| r) D_\kappa, \\ P_\kappa^F(r) &= \frac{|p_F|}{\sqrt{E + M_F}} r i_\kappa(|p_F| r) F_\kappa, & Q_\kappa^F(r) &= \sqrt{E + M_F} r i_{\kappa-1}(|p_F| r) F_\kappa, \end{aligned} \quad (\text{B.73})$$

for positive integer κ , and

$$\begin{aligned} P_{-\kappa}^D(r) &= -i\sqrt{E + M_D} r i_{-\kappa-1}(|p_D| r) D_{-\kappa}, & Q_{-\kappa}^D(r) &= i\frac{|p_D|}{\sqrt{E + M_D}} r i_{-\kappa}(|p_D| r) D_{-\kappa}, \\ P_{-\kappa}^F(r) &= \frac{|p_F|}{\sqrt{E + M_F}} r i_{-\kappa-1}(|p_F| r) F_{-\kappa}, & Q_{-\kappa}^F(r) &= \sqrt{E + M_F} r i_{-\kappa}(|p_F| r) F_{-\kappa}, \end{aligned} \quad (\text{B.74})$$

for negative integer $-\kappa$. Here, $p_{D,F}^2 = E^2 - M_{D,F}^2 < 0$. The coefficients of the wave functions for gluinos and the fermions inside the Q-ball are denoted by C_κ , D_κ , and F_κ .

As with the previous section, we match the wave functions at the boundary of the Q-ball located at $r = R$. We assume that the quarks are massless and that the mass of the other fermions is larger than the energy of the incoming quark. When the energy of the incoming quark is large such that $ER \gg 1$ and the gluino mass and the field value is sufficiently large such that $MR \gg 1$, we obtain $D_\kappa = 0$ and

$$A_\kappa = (-1)^\kappa i e^{2iER} B_\kappa, \quad A_{-\kappa} = (-1)^{-\kappa+1} i e^{2iER} B_{-\kappa}. \quad (\text{B.75})$$

There is an extra factor e^{2iER} in the relation between the amplitudes in contrast to the previous section. This is because the matching condition is imposed at $r = R$. Meanwhile, when the energy of the incoming quark is sufficiently small such that $ER \ll j$, one obtains $A_\kappa = B_\kappa$ and $C_\kappa = D_\kappa = F_\kappa = 0$.

Now, we will consider the physical interpretation of the relation among the wave functions above. For this purpose, we consider special linear combinations of the spinor that are proportional to the

Dirac spinor. The spinors for the incoming/outgoing massless quarks are written as

$$u_{\kappa,m}(\mathbf{r}, p) = \sqrt{4\pi p} \begin{pmatrix} -i f_{j+\frac{1}{2}}(pr) \Omega_{j,j+\frac{1}{2},m}(\theta, \phi) \\ f_{j-\frac{1}{2}}(pr) \Omega_{j,j-\frac{1}{2},m}(\theta, \phi) \end{pmatrix}, \quad (\text{B.76})$$

$$u_{-\kappa,m}(\mathbf{r}, p) = \sqrt{4\pi p} \begin{pmatrix} f_{j-\frac{1}{2}}(pr) \Omega_{j,j-\frac{1}{2},m}(\theta, \phi) \\ -i f_{j+\frac{1}{2}}(pr) \Omega_{j,j+\frac{1}{2},m}(\theta, \phi) \end{pmatrix}, \quad (\text{B.77})$$

where $f_j(pr)$ denotes the spherical Hankel functions $h_j^{(1,2)}(pr)$. Taking a specific linear combination and summing over κ , we get

$$u(\mathbf{p}, \chi_{\pm\frac{1}{2}}) f(pr, \cos \theta) = \sum_{\kappa=1}^{\infty} i^{\kappa-1} \sqrt{\kappa} \left[\pm u_{\kappa, \pm\frac{1}{2}}(\mathbf{r}, p) + u_{-\kappa, \pm\frac{1}{2}}(\mathbf{r}, p) \right]. \quad (\text{B.78})$$

Here, the spinor and the function are given by

$$u(\mathbf{p}, \chi_{\pm\frac{1}{2}}) = \sqrt{p} \begin{pmatrix} \chi_{\pm\frac{1}{2}} \\ \frac{\boldsymbol{\sigma} \cdot \mathbf{p}}{p} \chi_{\pm\frac{1}{2}} \end{pmatrix}, \quad f(pr, \cos \theta) = \sum_{\kappa=0}^{\infty} i^{\kappa} f_{\kappa}(pr) P_{\kappa}(\cos \theta). \quad (\text{B.79})$$

If we take f_{κ} to be the modified Bessel function j_{κ} , this is nothing but the partial-wave expansion of the plane wave. We use this linear combination as an incoming state, and one finds the coefficients for positive κ as

$$A_{\kappa} = \pm i^{\kappa-1} \sqrt{\kappa}, \quad A_{-\kappa} = i^{\kappa-1} \sqrt{\kappa}. \quad (\text{B.80})$$

When the energy of the incoming quark is sufficiently large, the relation between the coefficients is given by Eq. (B.75) and leads to

$$B_{\kappa} = \mp (-1)^{-\kappa} i e^{-2iER} i^{\kappa-1} \sqrt{\kappa}, \quad B_{-\kappa} = (-1)^{-\kappa} i e^{-2iER} i^{\kappa-1} \sqrt{\kappa}. \quad (\text{B.81})$$

The relative sign of B_{κ} and $B_{-\kappa}$ is opposite to that of A_{κ} and $A_{-\kappa}$. In other words, when the left-handed quark comes into the Q-ball, the right-handed anti-quark is reflected. Hence, we observe the similar results to the previous discussion even taking into account the spherical wave.

Meanwhile, when the energy of the incoming quark is sufficiently small such that $ER \ll j$, the relation between the amplitudes of the incoming quark and the outgoing quark is given by $A_{\kappa} = B_{\kappa}$. Thus, the relative sign of B_{κ} and $B_{-\kappa}$ is same as that of A_{κ} and $A_{-\kappa}$. When the left-handed quark comes into the Q-ball, the left-handed quark is reflected.

We find the solution as follows:

$$B_{\frac{1}{2}, \pm} = 0, \quad B_{-\frac{1}{2}, +} = i(-1)^{\kappa} \sqrt{\frac{E-2\omega}{E}} e^{-2i(E-\omega)R} A, \quad B_{-\frac{1}{2}, -} = 0, \quad (\text{B.82})$$

$$C_{\frac{1}{2}, \pm} = 0, \quad C_{-\frac{1}{2}, +} = 0, \quad C_{-\frac{1}{2}, -} = i^{\kappa} \frac{1-i}{2} \tan \beta \sqrt{\frac{M}{E}} e^{-iER} e^{MR} A, \quad (\text{B.83})$$

$$D_{m, \pm} = 0, \quad F_{\frac{1}{2}, \pm} = 0, \quad F_{-\frac{1}{2}, +} = 0, \quad F_{-\frac{1}{2}, -} = i^{\kappa} \frac{1-i}{\cos \beta} \sqrt{\frac{M}{E}} e^{-iER} e^{-M-R} A. \quad (\text{B.84})$$

C S -matrix for the Q-ball Scattering

We use the two-component spinors to describe the Majorana fermions inside the Q-ball and the Weyl fermions outside the Q-ball in (3+1)-dimensional spacetime, which correspond to the fermions with two degrees of freedom. In Section 2.1, we focus on the normal-incident scattering of the (colorless) quark on the infinitely-large Q-ball wall. The incoming quark may be regarded as the (1+1)-dimensional fermion for this scattering for $\theta = 0$: the fermions with two degrees of freedom in the (1+1)-dimension are the Dirac fermion.

Now, we discuss the correspondence between the fermions in terms of the (3+1)-dimension and in terms of the (1+1)-dimension. Let us assume that the fermions move along the z axis. We first consider the correspondence inside the Q-ball: the fermions are described by the Majorana fermions in terms of the (3+1)-dimension, while are described by the Dirac fermions in terms of the (1+1)-dimension. The Majorana fermions do not have any internal charges, but the Dirac fermions in terms of the (1+1)-dimension should have a kind of “charges”. The Majorana fermions have the up- and down-spin components, which get the opposite phase factors under the rotation around the z -axis. Meanwhile, since the fermions in the (1+1)-dimension do not feel the rotation around the z -axis, it is regarded as an internal symmetry. The Majorana fermion in the (3+1)-dimension is interpreted as the Dirac fermion in the (1+1)-dimension, which is composed of two degrees of freedom with the opposite “charges” arising from the spin degrees of freedom in the (3+1)-dimension.

We may consider the S -matrix structure of the one-dimensional scattering process. The S -matrix element is defined as the expansion of “in” state in terms of “out” state.

$$|a\rangle_{\text{in}} = \sum_{\beta} S_{ba} |b\rangle_{\text{out}}. \quad (\text{C.1})$$

Here, a, b denote the label of degrees of freedom.

We consider the one-dimensional scattering with $\omega = 0$. The “in” state is labelled by mass inside the Q-ball, helicity, and the moving direction. Since a massless fermion just passes through the Q-ball, its S -matrix elements are trivial. Moreover, the S -matrix is block-diagonalized with respect to the mass inside the Q-ball:

$$S' = \begin{pmatrix} \mathbf{1}_4 & 0 \\ 0 & S_4 \end{pmatrix}. \quad (\text{C.2})$$

We define the “in” state as a direct product of the mass eigenstates and the states labelled by the helicity and the moving direction. We choose the four-component basis consisting of the “in” states as

$$\begin{pmatrix} R+ \\ L- \\ R- \\ L+ \end{pmatrix}_{\text{in}}. \quad (\text{C.3})$$

Here, L, R denotes the moving direction, and \pm denotes the helicity $\pm 1/2$. In Section 2.1, we find that the right-moving quark is reflected as the left-moving anti-quark on the Q-ball boundary for $\theta = 0$. Let us assume that the semi-infinite Q-ball exists at $z > 0$ and its boundary is located at $z = 0$, which is the same system discussed in Ref. [17]. The coefficient of the reflected anti-quark is

given by $B = iA$, and hence ${}_{\text{out}}\langle L + |R-\rangle_{\text{in}} = i$ and other S -matrix elements associated with $|R-\rangle_{\text{in}}$ vanish.

We find the other matrix elements using the CP and T transformations. Under CP and time-reversal transformations, the “in” states transform as,

$$CP \begin{pmatrix} R+ \\ L- \\ R- \\ L+ \end{pmatrix}_{\text{in}} = i \begin{pmatrix} L- \\ R+ \\ L+ \\ R- \end{pmatrix}_{\text{in}}, \quad T \begin{pmatrix} R+ \\ L- \\ R- \\ L+ \end{pmatrix}_{\text{in}} = \begin{pmatrix} L+ \\ R- \\ -L- \\ -R+ \end{pmatrix}_{\text{out}}. \quad (\text{C.4})$$

Here, we take into account the intrinsic parity of the Majorana fermion to be $\eta = +i$ and the relative sign under the time-reversal (originating from $i\sigma_2$). Only four entries of S_4 are non-zero, and all of them are equal:

$$S_4 = i \begin{pmatrix} 0 & 1 & 0 & 0 \\ 1 & 0 & 0 & 0 \\ 0 & 0 & 0 & 1 \\ 0 & 0 & 1 & 0 \end{pmatrix}. \quad (\text{C.5})$$

This S -matrix is given in the mass basis inside Q-ball.

D Non-relativistic Scattering of Nucleons

From the discussions about scattering of colorless quarks on the Q-ball (with $\omega = 0$), one might naively expect that some of nucleons incident into the Q-ball is reflected as anti-nucleons. In particular, once the delta baryon, Δ^{++} or Δ^- , comes into Q-ball, it is expected that the delta baryon is totally reflected as its anti-baryon since they are spin-3/2 states and all spins of quarks inside are aligned. To begin with, we consider the one-dimensional non-relativistic scattering of nucleons on the (spherically symmetric) Q-ball in order to examine this behavior. The Schrödinger equation describes the non-relativistic scattering:

$$\left[-\frac{\nabla^2}{2m} + V_{\text{NR}} \right] \varphi(x) = E\varphi(x). \quad (\text{D.1})$$

Here, φ denotes the two-component wave function for nucleon and anti-nucleon:

$$\varphi = \begin{pmatrix} \varphi_N \\ \varphi_{\bar{N}} \end{pmatrix}. \quad (\text{D.2})$$

We assume that the center of the Q-ball locates at $x = 0$ and that its radius is R . The potential V_{NR} for this system is zero outside Q-ball ($|x| > R$). Meanwhile, along our discussion using the colorless toy model, the Q-ball has a uniform distribution and may affect the wave function for nucleons as a position-independent potential. This potential is parameterized by two parameters inside Q-ball ($|x| < R$):⁴

$$V_{\text{NR}} = V_0 \theta(R - |x|) \begin{pmatrix} 1 & \beta \\ \beta^* & 1 \end{pmatrix}. \quad (\text{D.3})$$

⁴In general, we can also include the boundary terms proportional to the delta function. The following discussion does not significantly change once we include them.

We assume CP invariance of the potential, and thus the diagonal components of the potential are same. The potential matrix is hermitian, and β can take a complex value. This complex phase can be absorbed by the phase rotation of wave function, and thus we simply assume the positive β in this study.

Now, we consider the situation where only a nucleon is coming from the left-side of the Q-ball. Outer region of the Q-ball, the wave functions are given by linear combinations of the free solutions:

$$\begin{aligned}\varphi_N(x) &= e^{ikx} + \bar{R}e^{-ikx}, & (x < -R), & & \varphi_{\bar{N}}(x) &= \tilde{R}e^{-ikx}, & (x < -R), \\ &= \bar{T}e^{ikx}, & (x > R), & & &= \tilde{T}e^{ikx}, & (x > R),\end{aligned}\quad (D.4)$$

where \bar{R} (\tilde{R}) denotes the reflection amplitude of nucleon (anti-nucleon), respectively, while \bar{T} (\tilde{T}) denotes each transmission amplitude. Meanwhile, the eigenfunctions inside the Q-ball are given by the linear combinations of the damping and growing solutions:

$$\varphi_{\pm}(x) = A_{\pm}e^{-\kappa_{\pm}x} + B_{\pm}e^{\kappa_{\pm}x}, \quad (D.5)$$

where $\kappa_{\pm}^2 = -k^2 + 2mV_0(1 \pm \beta)$. We assume $\kappa_{\pm} > 0$ in order that there is no propagating mode in the Q-ball, since we are interested in a solution with nucleon being totally reflected as anti-nucleon. Matching the wave functions and their derivatives with respect to x at $x = R, -R$, one finds the solutions for the matching conditions in the large $\kappa_{\pm}R$ limit as follows.

$$\bar{R} = -\frac{1}{2} \left(\frac{ik + \kappa_+}{-ik + \kappa_+} + \frac{ik + \kappa_-}{-ik + \kappa_-} \right) e^{-2ikR}, \quad \tilde{R} = -\frac{1}{2} \left(\frac{ik + \kappa_+}{-ik + \kappa_+} - \frac{ik + \kappa_-}{-ik + \kappa_-} \right) e^{-2ikR}, \quad (D.6)$$

$$\bar{T} = 2ike^{-2ikR} \left[\frac{e^{-2\kappa_+R}\kappa_+}{(k + i\kappa_+)^2} + \frac{e^{-2\kappa_-R}\kappa_-}{(k + i\kappa_-)^2} \right], \quad \tilde{T} = 2ike^{-2ikR} \left[\frac{e^{-2\kappa_+R}\kappa_+}{(k + i\kappa_+)^2} - \frac{e^{-2\kappa_-R}\kappa_-}{(k + i\kappa_-)^2} \right], \quad (D.7)$$

$$A_{\pm} = \pm\sqrt{2}e^{-\kappa_{\pm}R}e^{-ikR}\frac{k}{k + i\kappa_{\pm}}, \quad B_{\pm} = \mp\sqrt{2}e^{-3\kappa_{\pm}R}e^{-ikR}\frac{k(k - i\kappa_{\pm})}{(k + i\kappa_{\pm})^2}. \quad (D.8)$$

If nucleon incident the Q-ball is completely reflected as anti-nucleon at the boundary, the reflection amplitude for nucleon vanishes (namely $\bar{R} = 0$) and thus $k^2 + \kappa_+\kappa_- = 0$. However, the left hand side, $k^2 + \kappa_+\kappa_-$, is always positive, and hence the reflection amplitude for nucleon never vanishes in this model. Meanwhile, in the range of $\kappa_- < k < \kappa_+$ (keeping κ_-R large), the reflection amplitude for anti-nucleon is comparable with that for nucleon. This is realized for a large range of k when $\beta \simeq 1$. To further extend the range of k , we also consider the case where there is a propagating mode inside Q-ball. The solution in the large κ_+R limit is approximately given by

$$\bar{R} + \tilde{R} \simeq -e^{-2ikR}, \quad \bar{R} - \tilde{R} \simeq \frac{(k^2 - k_-^2)(e^{4ik_-R} - 1)e^{-2ikR}}{(e^{4ik_-R} - 1)k^2 - 2(e^{4ik_-R} + 1)kk_- + (e^{4ik_-R} - 1)k_-^2}, \quad (D.9)$$

$$\bar{T} + \tilde{T} \simeq -\frac{4ike^{-2ikR}e^{-2\kappa_+R}}{\kappa_+}, \quad \bar{T} - \tilde{T} \simeq -\frac{4ikk_-e^{-2i(k-k_-)R}}{(k - k_-)^2e^{4ik_-R} - (k + k_-)^2}, \quad (D.10)$$

$$A_+ = -\sqrt{2}ie^{-\kappa_+R}e^{-ikR}\frac{k}{\kappa_+}, \quad A_- = -\sqrt{2}\frac{e^{-i(k-3k_-)R}k(k - k_-)}{(k - k_-)^2e^{4ik_-R} - (k + k_-)^2}, \quad (D.11)$$

$$B_+ = -\sqrt{2}ie^{-3\kappa_+R}e^{-ikR}\frac{k}{\kappa_+}, \quad B_- = -\sqrt{2}\frac{e^{-i(k-k_-)R}k(k + k_-)}{(k - k_-)^2e^{4ik_-R} - (k + k_-)^2}, \quad (D.12)$$

where $k_-^2 = k^2 + 2mV_0(\beta - 1) > 0$. If $k_- \gg k$, the reflection amplitudes for anti-nucleon is suppressed. On the other hand, when $k_- \simeq k$, the reflection amplitudes for nucleon and for anti-nucleon are almost close to each other, $|\bar{R}| \simeq |\tilde{R}| \simeq 1/2$, and the transmitted amplitudes for them also have the same absolute value, $|\bar{T}| \simeq |\tilde{T}| \simeq 1/2$. In particular, $\beta = 1$ is an interesting choice where $k_- = k$ and the amplitude $|\tilde{R}|$ is comparable with the others for any k .

Furthermore, we examine how the above observation in one-dimensional scattering is realized in three-dimensional scattering. We also note that unlike quark (inside nucleon) scattering, one-dimensional analysis is not justified for nucleon scattering since kR can be smaller than unity, namely, Q-ball cannot be regarded as a wall for low-velocity nucleon. Under the spherical potential, the radial Schrödinger equation is given by

$$\left[-\frac{1}{2mr^2} \frac{d}{dr} \left(r^2 \frac{d}{dr} \right) + \frac{\ell(\ell+1)}{2mr^2} + V_{\text{NR}}(r) \right] \varphi(r) = E\varphi(r), \quad (\text{D.13})$$

with the constant spherical potential inside Q-ball

$$V_{\text{NR}}(r) = V_0 \theta(R - r) \begin{pmatrix} 1 & \beta \\ \beta^* & 1 \end{pmatrix}. \quad (\text{D.14})$$

Here, we again take β to be positive. The wave functions for the system are given by linear combinations of free solutions for outer region of the Q-ball as follows:

$$\varphi_N(r) = A h_\ell^{(2)}(kr) + \bar{R} h_\ell^{(1)}(kr), \quad (\text{D.15})$$

$$\varphi_{\bar{N}}(r) = \tilde{R} h_\ell^{(1)}(kr), \quad (\text{D.16})$$

Here, $h_\ell^{(1,2)}(x)$ is the spherical Hankel functions.

Let us start with the case where there is no propagating mode inside the Q-ball. The eigenfunctions inside the Q-ball are given by the modified spherical Hankel functions, which is regular at the origin.

$$\varphi_\pm(r) = A_\pm i_\ell(\kappa_\pm r), \quad (\text{D.17})$$

with the parameters κ_\pm which are the same as before: $\kappa_\pm^2 = -k^2 + 2mV_0(1 \pm \beta)$. By the matching conditions for wave functions and their derivative at $r = R$, we find the coefficients as follows.

$$\bar{R} + \tilde{R} = -\frac{ki_\ell(\kappa_+ R) h_\ell^{(2)'}(kR) - \kappa_+ i_\ell'(\kappa_+ R) h_\ell^{(2)}(kR)}{ki_\ell(\kappa_+ R) h_\ell^{(1)'}(kR) - \kappa_+ i_\ell'(\kappa_+ R) h_\ell^{(1)}(kR)} A, \quad (\text{D.18})$$

$$\bar{R} - \tilde{R} = -\frac{ki_\ell(\kappa_- R) h_\ell^{(2)'}(kR) - \kappa_- i_\ell'(\kappa_- R) h_\ell^{(2)}(kR)}{ki_\ell(\kappa_- R) h_\ell^{(1)'}(kR) - \kappa_- i_\ell'(\kappa_- R) h_\ell^{(1)}(kR)} A, \quad (\text{D.19})$$

and

$$A_\pm = -\frac{1}{\sqrt{2}} \frac{h_\ell^{(1)}(kR) h_\ell^{(2)'}(kR) - h_\ell^{(1)'}(kR) h_\ell^{(2)}(kR)}{ki_\ell(\kappa_\pm R) h_\ell^{(1)'}(kR) - \kappa_\pm i_\ell'(\kappa_\pm R) h_\ell^{(1)}(kR)} A. \quad (\text{D.20})$$

At large $\kappa_{\pm}R$, we find the approximate forms of the solutions as follows.

$$\bar{R} + \tilde{R} \simeq -\frac{h_{\ell}^{(2)}(kR) - \frac{kR}{\kappa_+R}h_{\ell}^{(2)'}(kR)}{h_{\ell}^{(1)}(kR) - \frac{kR}{\kappa_+R}h_{\ell}^{(1)'}(kR)}A, \quad (\text{D.21})$$

$$\bar{R} - \tilde{R} \simeq -\frac{h_{\ell}^{(2)}(kR) - \frac{kR}{\kappa_-R}h_{\ell}^{(2)'}(kR)}{h_{\ell}^{(1)}(kR) - \frac{kR}{\kappa_-R}h_{\ell}^{(1)'}(kR)}A. \quad (\text{D.22})$$

The reflection amplitude for anti-nucleon, \tilde{R}/A is suppressed by k/κ_- (for $kR \gg 1$) or $1/\kappa_-R$ (for $kR \ll 1$) compared to elastic amplitude $\bar{R}/A - 1$. Therefore, conversion (partial-wave) cross section

$$\tilde{\sigma}_{\ell} = \frac{\pi}{k^2}(2\ell + 1) \left| \frac{\tilde{R}}{A} \right|^2, \quad (\text{D.23})$$

is suppressed by $(k/\kappa_-)^2$ or $1/(\kappa_-R)^2$ compared to elastic (partial-wave) cross section

$$\bar{\sigma}_{\ell} = \frac{\pi}{k^2}(2\ell + 1) \left| \frac{\bar{R}}{A} - 1 \right|^2 \quad (\text{D.24})$$

as in the one-dimensional case. Therefore, we again consider the case where $\beta \simeq 1$ and also there is a propagating mode inside the Q-ball. The wave function $\varphi_-(r)$ is regular at the origin, and thus is given by $\varphi_-(r) = A_-j_{\ell}(k_-r)$. In this case, the solution is modified as follows.

$$\bar{R} - \tilde{R} = -\frac{kj_{\ell}(k_-R)h_{\ell}^{(2)'}(kR) - k_-j'_{\ell}(k_-R)h_{\ell}^{(2)}(kR)}{kj_{\ell}(k_-R)h_{\ell}^{(1)'}(kR) - k_-j'_{\ell}(k_-R)h_{\ell}^{(1)}(kR)}A, \quad (\text{D.25})$$

$$A_- = -\frac{1}{\sqrt{2}}\frac{h_{\ell}^{(1)}(kR)h_{\ell}^{(2)'}(kR) - h_{\ell}^{(1)'}(kR)h_{\ell}^{(2)}(kR)}{kj_{\ell}(k_-R)h_{\ell}^{(1)'}(kR) - k_-j'_{\ell}(k_-R)h_{\ell}^{(1)}(kR)}A. \quad (\text{D.26})$$

Here, $k_-^2 = k^2 + 2mV_0(\beta - 1)$.

Lastly, we show the approximate forms of the reflection amplitudes in $kR \gg 1$ and $kR \ll 1$ limits with keeping k/κ_+ small. The reflection amplitudes in the high-energy limit, $kR \gg 1$, are approximated as follows.

$$\bar{R} + \tilde{R} \simeq \left(1 + \frac{2ikR}{\kappa_+R}\right)e^{-2ikR+i\ell\pi}A, \quad \bar{R} - \tilde{R} \simeq \frac{k_-j'_{\ell}(k_-R) + ikj_{\ell}(k_-R)}{k_-j'_{\ell}(k_-R) - ikj_{\ell}(k_-R)}e^{-2ikR+i\ell\pi}A. \quad (\text{D.27})$$

If $k_- \gg k$, the conversion amplitude is suppressed by k/k_- compared to the elastic amplitude. On the other hand, when $k_- \simeq k$,

$$\bar{R} \simeq \frac{e^{-2ikR+i\ell\pi} + 1}{2}A, \quad \tilde{R} \simeq \frac{e^{-2ikR+i\ell\pi} - 1}{2}A, \quad (\text{D.28})$$

and thus conversion and elastic cross sections are equal and given by a quarter of hard-sphere scattering cross section. The reflection amplitudes in the low-energy limit, $kR \ll 1$, with keeping the

leading order of $\kappa_+ R$ corrections are expanded as follows.

$$\bar{R} + \tilde{R} \simeq A - \frac{2i(kR)^{2\ell+1}}{(2\ell+1)!} \left(1 - \frac{2\ell+1}{\kappa_+ R}\right) A, \quad (\text{D.29})$$

$$\bar{R} - \tilde{R} \simeq A - \frac{2i(kR)^{2\ell+1}}{(2\ell+1)!} \frac{k_- R j'_\ell(k_- R) - \ell j_\ell(k_- R)}{k_- R j'_\ell(k_- R) + (\ell+1) j_\ell(k_- R)} A. \quad (\text{D.30})$$

If $k_- R \gg 1$, the conversion amplitude is suppressed by $1/(k_- R)$ compared to the elastic amplitude. On the other hand, when $k_- R \ll 1$,

$$\bar{R} \simeq A - \frac{i(kR)^{2\ell+1}}{(2\ell+1)!} A, \quad \tilde{R} \simeq -\frac{i(kR)^{2\ell+1}}{(2\ell+1)!} A. \quad (\text{D.31})$$

and thus conversion and elastic cross sections are equal and given by a quarter of hard-sphere scattering cross section. We note that $\beta = 1$ is an interesting choice, where conversion and elastic cross sections are comparable for any k as in the one dimensional case.

References

- [1] S. Kasuya, M. Kawasaki, and T. T. Yanagida, “IceCube potential for detecting Q-ball dark matter in gauge mediation,” *PTEP* **2015** no. 5, (2015) 053B02, [arXiv:1502.00715 \[hep-ph\]](#).
- [2] G. Rosen, “Particlelike Solutions to Nonlinear Complex Scalar Field Theories with Positive-Definite Energy Densities,” *J. Math. Phys.* **9** (1968) 996.
- [3] R. Friedberg, T. D. Lee, and A. Sirlin, “A Class of Scalar-Field Soliton Solutions in Three Space Dimensions,” *Phys. Rev. D* **13** (1976) 2739–2761.
- [4] S. R. Coleman, “Q-balls,” *Nucl. Phys. B* **262** no. 2, (1985) 263. [Addendum: *Nucl. Phys. B* 269, 744 (1986)].
- [5] A. Kusenko, “Solitons in the supersymmetric extensions of the standard model,” *Phys. Lett. B* **405** (1997) 108, [arXiv:hep-ph/9704273](#).
- [6] A. Kusenko and M. E. Shaposhnikov, “Supersymmetric Q balls as dark matter,” *Phys. Lett. B* **418** (1998) 46–54, [arXiv:hep-ph/9709492](#).
- [7] T. Gherghetta, C. F. Kolda, and S. P. Martin, “Flat directions in the scalar potential of the supersymmetric standard model,” *Nucl. Phys. B* **468** (1996) 37–58, [arXiv:hep-ph/9510370](#).
- [8] M. Dine, L. Randall, and S. D. Thomas, “Baryogenesis from flat directions of the supersymmetric standard model,” *Nucl. Phys. B* **458** (1996) 291–326, [arXiv:hep-ph/9507453](#).
- [9] A. G. Cohen, S. R. Coleman, H. Georgi, and A. Manohar, “The Evaporation of Q Balls,” *Nucl. Phys. B* **272** (1986) 301–321.
- [10] M. Kawasaki and M. Yamada, “Q ball Decay Rates into Gravitinos and Quarks,” *Phys. Rev. D* **87** no. 2, (2013) 023517, [arXiv:1209.5781 \[hep-ph\]](#).

- [11] M. Kawasaki and H. Nakatsuka, “Q-ball decay through A-term in the gauge-mediated SUSY breaking scenario,” *JCAP* **04** (2020) 017, [arXiv:1912.06993 \[hep-ph\]](#).
- [12] S. Kasuya, M. Kawasaki, and N. Tsuji, “MeV gamma rays from Q-ball decay,” *Phys. Rev. D* **109** no. 8, (2024) 083039, [arXiv:2403.01675 \[hep-ph\]](#).
- [13] A. Kusenko, M. E. Shaposhnikov, P. G. Tinyakov, and I. I. Tkachev, “Star wreck,” *Phys. Lett. B* **423** (1998) 104–108, [arXiv:hep-ph/9801212](#).
- [14] A. Kusenko, V. Kuzmin, M. E. Shaposhnikov, and P. G. Tinyakov, “Experimental signatures of supersymmetric dark matter Q balls,” *Phys. Rev. Lett.* **80** (1998) 3185–3188, [arXiv:hep-ph/9712212](#).
- [15] **Super-Kamiokande** Collaboration, Y. Takenaga *et al.*, “Search for neutral Q-balls in super-Kamiokande II,” *Phys. Lett. B* **647** (2007) 18–22, [arXiv:hep-ex/0608057](#).
- [16] T. Multamaki and I. Vilja, “Analytical and numerical properties of Q balls,” *Nucl. Phys. B* **574** (2000) 130–152, [arXiv:hep-ph/9908446](#).
- [17] A. Kusenko, L. Loveridge, and M. Shaposhnikov, “Supersymmetric dark matter Q-balls and their interactions in matter,” *Phys. Rev. D* **72** (2005) 025015, [arXiv:hep-ph/0405044](#).
- [18] A. K. Drukier, S. Baum, K. Freese, M. Górski, and P. Stengel, “Paleo-detectors: Searching for Dark Matter with Ancient Minerals,” *Phys. Rev. D* **99** no. 4, (2019) 043014, [arXiv:1811.06844 \[astro-ph.CO\]](#).
- [19] S. Baum *et al.*, “Mineral detection of neutrinos and dark matter. A whitepaper,” *Phys. Dark Univ.* **41** (2023) 101245, [arXiv:2301.07118 \[astro-ph.IM\]](#).
- [20] J. Arafune, T. Yoshida, S. Nakamura, and K. Ogure, “Experimental bounds on masses and fluxes of nontopological solitons,” *Phys. Rev. D* **62** (2000) 105013, [arXiv:hep-ph/0005103](#).
- [21] I. M. Shoemaker and A. Kusenko, “The Ground states of baryoleptonic Q-balls in supersymmetric models,” *Phys. Rev. D* **78** (2008) 075014, [arXiv:0809.1666 \[hep-ph\]](#).
- [22] J.-P. Hong, M. Kawasaki, and M. Yamada, “Charged Q-ball Dark Matter from B and L direction,” *JCAP* **08** (2016) 053, [arXiv:1604.04352 \[hep-ph\]](#).
- [23] J.-P. Hong and M. Kawasaki, “New type of charged Q -ball dark matter in gauge mediated SUSY breaking models,” *Phys. Rev. D* **95** no. 12, (2017) 123532, [arXiv:1702.00889 \[hep-ph\]](#).
- [24] **IceCube** Collaboration, M. G. Aartsen *et al.*, “The IceCube Neutrino Observatory Part IV: Searches for Dark Matter and Exotic Particles,” in *33rd International Cosmic Ray Conference*. 9, 2013. [arXiv:1309.7007 \[astro-ph.HE\]](#).
- [25] Y. Almumin, J. Heeck, A. Rajaraman, and C. B. Verhaaren, “Slowly rotating Q-balls,” *Eur. Phys. J. C* **84** no. 4, (2024) 364, [arXiv:2302.11589 \[hep-th\]](#).

- [26] J. J. Sakurai and J. Napolitano, *Modern Quantum Mechanics*. Quantum physics, quantum information and quantum computation. Cambridge University Press, 3 ed., 10, 2020.
- [27] K. Enqvist and J. McDonald, “Q balls and baryogenesis in the MSSM,” *Phys. Lett. B* **425** (1998) 309–321, [arXiv:hep-ph/9711514](#).
- [28] J. Hisano, M. M. Nojiri, and N. Okada, “The Fate of the B ball,” *Phys. Rev. D* **64** (2001) 023511, [arXiv:hep-ph/0102045](#).
- [29] I. A. Kotelnikov and A. I. Milstein, “Electron radiative recombination with a hydrogen-like ion,” *Physica Scripta* **94** no. 5, (2019) 055403, [1810.08071](#).
- [30] L. D. Landau and E. M. Lifshits, *Quantum Mechanics: Non-Relativistic Theory*, vol. v.3 of *Course of Theoretical Physics*. Butterworth-Heinemann, Oxford, 1991.
- [31] V. B. Berestetskii, E. M. Lifshitz, and L. P. Pitaevskii, *Quantum Electrodynamics*. Course of Theoretical Physics. 1982.
- [32] W. R. Johnson, *Atomic structure theory*. Springer, 2007.